Surface water flow resistance due to emergent wetland vegetation

Karen Leigh Hall

Thesis submitted to the faculty of the Virginia Polytechnic Institute and State University
in partial fulfillment of the requirements for the degree of

Master of Science
in
Biological Systems Engineering

Theresa M. Thompson
Panayiotis Diplas
Zachary M. Easton

April 11, 2012
Blacksburg, VA

Keywords: vegetation, flow, resistance, friction factor, wetland

Surface water flow resistance due to emergent wetland vegetation

Karen Leigh Hall

ABSTRACT

The key to a successful wetland design is duplicating the hydroperiod of the desired wetland type. Dense wetland vegetation affects surface water flow rates by increasing flow resistance. Prior research represented the vegetation as individual stems; however, many wetland species grow in clumps. Therefore, the objectives of this study were to investigate the effect of clumping vegetation on flow resistance and to develop a prediction equation for use in wetland design. A 6-m by 1-m by 0.4-m recirculating flume was planted with mature common rush, *Juncus effusus*, a common emergent wetland plant. Three different flow rates (3, 4, and 5 L/s) and three different tailgate heights (0, 2.5, and 5 cm) were used to simulate a variety of wetland conditions. Plant spacing and clump diameter were varied (20 and 25 cm, 8 and 12 cm, respectively). Friction factors ranged from 9 to 40 and decreased with increasing plant density. Non-dimensional parameters determined through Buckingham Pi analysis were used in a regression analysis to develop a prediction model. Results of the regression analysis showed that the fraction of vegetated occupied area (P) was most significant factor in determining friction factor.

Dedication

I dedicate this to Maggie Moyler. I have thought about her every day since she left this world, and every day I wish I could bring her back for my sake and everyone else that loved her so much.

Rest in peace, Love.

Acknowledgments

I want to thank everyone that helped me with my research. My advisor, Theresa Thompson, has been nothing but assuring and supportive throughout this entire process. I appreciate the opportunity I get my Masters in a year and she guided me through it even though the hardest times.

I would like to thank my committee, Panos Diplas and Zach Easton. Dr. Diplas always shared his thoughts and gave advice, which was greatly appreciated. Dr. Easton even though he was on the other side of Virginia always made himself available whenever needed via email, Sykpe, or very long drive.

I would also like to thank Laura Teany for always being there. I don't even know anymore how many times she took the point gage apart, but each and every time was greatly appreciated. All her advice on how to handle different situations and always making herself available to moving dirt or getting batteries was such a huge help.

My fiancé, Chris Propst, also needs to be thanked for spending a few weekends in the lab with me and helping me. His support was so helpful, and those long weekends spent in the lab would not have been as good without him around. Also, Waverly Parks, Janell Henry, and Eric Neuhaus for helping me in the middle of August digging up plants and planting them in the lab. I literally don't know how long that would have taken me without their help and I may have also thrown my back out.

Anyone who helped me at all this year I have to thank. My family's support and confidence in me was always so helpful and there when I needed it.

Table of Contents

List of Figures

List of Tables

Chapter 1. Introduction

Wetlands are natural ecosystems that are important for nutrient cycling and flood mitigation. Approximately 54% of the wetlands in the United States have been lost due to a variety of reasons, from agriculture to transportation. Wetlands were filled and drained without regulatory oversight until the Federal Water Pollution Control Act of 1972. Section 404 of the act requires permitting for dredging or filling of waters of the state. In 1989, United States adopted a "no net loss" policy for wetlands. The Army Corps of Engineers (Corps) and EPA have regulatory oversight for Section 404; The Corps enforces the policy with a four-step approach to wetland management: avoidance, minimization, on-site compensation, and finally mitigation.

Wetland mitigation is the creation of a wetland to replace wetlands that are destroyed due to human activity. Mitigation of a lost wetland must be "type-for–type" and within the same region as the original wetland. For example, if a freshwater, tidal, forested wetland is destroyed, the replacement wetland must also be a freshwater tidal, forested wetland, ideally in the same watershed. Because new wetlands do not have the same level of ecosystem services as established wetlands, replacement at a greater spatial extent is frequently mandated. A mitigation ratio is the ratio of the acreage of required mitigation wetlands to the acreage of destroyed wetlands. Forested wetlands have lower rates of mitigation success and high levels of ecosystem services, so the amount of acreage needed for replacement can be two to three times the acreage that is destroyed. For example Maryland requires mitigation at a 3:1 ratio for forested nontidal wetlands (Crookshank and American Petroleum, 1995).

Hydrology is the first step to successful wetland mitigation; many wetlands fail because they are too wet or dry. An investigation conducted on wetland projects around Chicago, IL, USA determined 52% of local created wetlands had unplanned open water and another 9% were too dry (National Research Council. Committee on Mitigating Wetland, 2001).

Wetland hydrology has several components that need to be taken into consideration when designing constructed wetlands. Inflows and outflows are modeled and manipulated to meet the hydrology criteria. While some factors, such as precipitation, cannot be engineered, ground water inflows and outflows can be controlled with a clay liner, surface flow outflows can be controlled with designed outflow structures, and surface water inflows can be manipulated with inflow structures or berms.

One key influence on wetland hydrology is vegetation. In open channels, flow resistance is due to boundary resistance, but in wetlands, flow resistance is largely due to the vegetation. Bennett and Simon (2004) found as the density of the plant community increases, water depth increases, and velocities decrease. Also, turbulent activity, such as surface waves, flow separation, and vertical structures, increase and become more apparent within the vegetated flow area. Currently, the impact of wetland vegetation on surface flow resistance is not considered in wetland design. Engineers commonly assume the outlet structure controls outflow from the wetland; however, roughness in dense wetland vegetation can influence the slope of the water surface which would change the water surface elevation.

Multiple studies have analyzed the impact of vegetation on surface flows, but prediction equations have not been developed for use in design. Typically vegetation

studies are conducted using dowels and are modeled using individual stems (Bennett and Simon, 2004; Liu et al., 2008; Nepf, 1999). However, typical emergent wetland vegetation, such as *Juncus effusus,* grows in a tufted or clumped pattern. This clumped pattern alters the effective radius of the plant because the stems create one dense cylinder. Species, like rush, are commonly seeded in new wetlands to provide ground cover; thus, emergent wetlands dominated by these herbaceous species are not uncommon. The goal of this study is to develop an equation to predict friction factor in emergent wetlands for use in mitigation wetland design. Specific objectives are as follows:

- To evaluate the significance of clumping relative to other vegetative parameters, such as stem diameter; and,
- To develop an improved prediction equation.

Chapter 2. Literature Review

What Are Wetlands?

Wetlands are important ecosystems that can take a variety of forms. Several terms are used to describe different kinds of wetlands such as, swamp, slough, marsh, bog, billabong, fen, mire, and moor (Mitsch and Gosselink, 2000). Wetlands have even been legally defined by the Food Security Act as a result of the *swampbuster provision.* Title 16 § 3801 (a)(18) states the following:

> "The term 'wetland', except when such term is part of the term 'converted wetland', means land that—
>
> (A) has a predominance of hydric soils;
>
> (B) is inundated or saturated by surface or groundwater at a frequency and duration sufficient to support a prevalence of hydrophytic vegetation typically adapted for life in saturated soil conditions; and
>
> (C) under normal circumstances does support a prevalence of such vegetation."

Even with a legal definition, wetlands can be difficult to delineate. Currently, more than 50 definitions (Dugan et al., 1993) exist to describe the different types of wetlands that occur on every continent except Antarctica. No one definition satisfies every occurrence. Different types of wetlands can have different hydrological characteristics. Flood duration and flood frequency can change depending on where a wetland is located in the landscape. For instance, coastal wetlands are tidally influenced, with water levels that vary throughout the day, while wetlands that are more influenced

by groundwater have water levels that vary seasonally. Water levels in prairie pothole wetlands fluctuate in response to precipitation. Similarly, riverine wetlands are only inundated when the adjacent river floods (Mitsch and Gosselink, 2000).

Wetland Value

Wetlands are important ecosystems that reduce flooding, improve water quality, and provide habitat. A case study in Momoge National Natural Reserve, China compared the flood-holding capacity of wetland soils within the reserve to a reservoir with an equivalent flood storage capacity. Based on reservoir construction cost, the value of the wetlands was \$5,700 USD/hm^2/yr (Jiang et al., 2007).

Another beneficial characteristic of wetlands is that the water in wetlands moves slowly, allowing sediment to drop out before the water exits the wetland and continues downstream. The sediment load in runoff from a potato field in Northern Maine was reduced 90 to 100% due to dense wetland vegetation in an emergent marsh (Donald A, 1992). Wetlands can also improve water quality via nutrient uptake by wetland plants.

Additionally, wetlands provide a unique habitat for fish, birds, and mammals. Of the commercial fish species in the United States, 95% of them live some part of their life cycle in wetlands (Mitsch and Gosselink, 2000). Wetlands are important to species preservation as well. Half of the species on the United States endangered list make their homes in wetlands (Mitsch and Gosselink, 2000).

Wetland Loss

Due to the expansion of agricultural and urban lands, wetlands were drained and filled. Wetland loss in the United States alone is estimated to be 54%. Levees, ditches,

and canals have been constructed throughout the U.S. to drain wetlands for various reasons, from agriculture to transportation and construction (Mitsch and Gosselink, 2000). Eighty percent of that loss is a result of agricultural use (Dugan et al., 1993).

According to Dahl (1990), 22 states lost at least 50% of their wetland acreage or more between 1780 and 1980. Florida alone lost 9.3 million acres in the same time period. California has the greatest amount of wetland loss with 91% lost since the 1780's. From the 1970's to the 1980's alone, 3.4 million acres of forested wetlands were destroyed throughout the U.S. (Dahl et al., 1991). In a study of Status and Trends of Wetlands in the Conterminous United States from 2004 to 2009 for the U.S. Fish and Wildlife Service, Dahl (2011) showed increases in shrub, emergent, and intertidal wetlands; however, the overall acreage of wetlands decreased from 2004 to 2009 by 0.1%. Forested and estuarine vegetated intertidal wetlands decreased by 1.2 and 2.4%, respectively, between 2004 and 2009. While the rate of wetland destruction has slowed overall, depletion of some wetland types continues.

Wetland Legislation

No one specific law protects wetlands in the United States. Section 404 of the Federal Water Pollution Control Act of 1972 stated no one could dredge or fill waters of the state without proper permitting. In 1977, an amendment was added that included wetlands in the definition of waters of the United States (Strand et al., 2009). In 1985, a provision of the Food Security Act in 1985, known as the "swampbuster" provision, stated that any farmer who knowingly destroyed a wetland in any one year period would be denied government aid (Mitsch and Gosselink, 2000). Because of the extensive loss of wetlands, the United States adopted a "no net loss" policy in 1989. This means that if a

delineated wetland was destroyed a new wetland must be constructed as a replacement. Section 404 of the Clean Water Act remains the main mechanism by which wetlands are protected in the U.S.

Currently, the standards and methods for delineating wetlands are described in the 1987 Corps Delineation manual. The manual defines methods on how to determine sufficient hydrology, soils, and vegetation to delineate a jurisdictional wetland. The manual does require some expertise to use however, because the manual only outlines allowable methods to determine if a site is a wetland (Strand et al., 2009).

When a wetland is defined and development is planned, a permit must be submitted. Most permits come in two different forms, either Nationwide or Individual. Nationwide permits are more flexible, but the development cannot exceed a minimum amount of disturbance. If the disturbance is more than the Nationwide permit will allow then an Individual permit must be submitted. These permits are overseen by EPA and allow for "public interest review" and allow EPA to set standards that must be met for each permit. Individual permits also allow EPA to override decisions made by the Corps (Strand et al., 2009).

Because there is no law specifically protecting wetlands in the US, case law has defined Clean Water Act jurisdiction over wetlands. The decision of the court in *Natural Resoucres Defense Council v. Callaway* (1975) stated that the U.S. Army Corps of Engineers was applying the Clean Water Act too narrowly, and, as a result, the Corps revised the definition from only "navigable waters" to include wetlands and isolated waters. More recent court cases have called into question the Corps' expanded definition of "waters," such as the *Rapanos* decision, where the Court reversed prosecutions made

for filling wetlands that were adjacent to non-navigable tributaries. The Court claimed that a flowing hydrologic connection or "significant nexus" to navigable water must exist for wetlands to be considered waters of the state (Strand et al., 2009).

Section 404 of the Federal Water Pollution Control Act states that a requirement of permitting may be reconstruction and restoration, which is the clause that allows the "no net loss" policy to be enforced. To maintain the amount of wetlands that currently exist, wetland mitigation banks have been developed to replace destroyed wetlands. The US Army Corp of Engineers has set up methods for delineating wetlands, so that 404 permitting can be enforced. Guidelines must be met before a 404 permit can be awarded. First, impacting the wetland should be avoided altogether if another alternative exists. Second, if the impacted area cannot be completely avoided then steps should be taken to minimize the impact as much as practically possible. Finally, any area that is impacted must be offset with wetland creation, enhancement, or restoration (National Research Council . Committee on Mitigating Wetland, 2001).

Policies for replacing wetlands vary from state to state and also can depend on the type of wetland being replaced. In Maryland, wetland replacement ratios vary from 1:1 to 3:1. The ratio of replacement depends only on the type of wetland being destroyed. Emergent nontidal wetlands require 1:1 replacement ratio while forested nontidal wetlands must be replaced at a 3:1 ratio. In contrast, Florida does not have a standard ratio for each type of wetland. Instead, the replacement ratio depends on site hydrology and existing vegetation at both the mitigation site and the destroyed wetland (Crookshank and American Petroleum, 1995).

Wetland mitigation can be done by the individual causing the wetland disturbance or, as an alternative, credits can be purchased from a wetland mitigation bank. A mitigation bank, according to the EPA, is a "wetland, stream, or other aquatic resource area that has been restored, established, enhanced, or (in certain circumstances) preserved for the purpose of providing compensation for unavoidable impacts." The value of a mitigation bank is defined by the credit type and the number of acres. The benefit of mitigation banking is that compensation is done by a third party; thus, the liability for the mitigation of the disturbance is transferred to the bank holders. Establishment of mitigation banks require a previous agreement with a regulatory agency and extensive post-construction monitoring.

Wetland mitigation sites are designed to replace the ecosystem services provided by destroyed or degraded wetlands; however, current designs limit how well a created wetland performs. An investigation conducted on wetland projects around Chicago, IL, USA determined 52% of local created wetlands had unplanned open water and another 9% were too dry (National Research Council . Committee on Mitigating Wetland, 2001). At one project in the study area, 29 ha required for the 404 permit were never constructed, and 99 ha were either too wet or dry to develop wetland conditions, resulting in a net loss of wetlands.

Mitigation wetlands can differ from reference wetlands in vegetation composition and hydrology. In a comparison of three mitigation wetlands to reference wetlands Cummings (1999) found that soil activity and composition in the mitigation wetlands did not resemble the reference wetlands. Over the five-year study period carbon levels either remained the same or decreased in the mitigation wetlands. The reference wetlands

contained a profile of carbon in the soil where, as the soil depth increased, the carbon levels decreased. Also, the soil pH at the constructed sites was significantly higher than at the reference sites.

Hydrologic functioning of constructed wetlands is also inconsistent compared to reference wetlands. Because hydrology defines wetland function and type, designing the proper wetland hydrology is important, but often overlooked (Garbisch, 2002). Created wetlands are typically wetter than the reference wetland used for design, and are inundated for longer periods than the reference wetlands (Cole and Brooks, 2000). Also, the hydroperiod of created wetlands is typically not as dynamic as in natural wetlands. Too much or too little water can cause changes in vegetation species composition; wetland diversity is linked to how wetlands function hydrologically. The amount of water in a wetland influences the species of plants and animals that will thrive (Maltby et al., 2009). Long term inundation would not be suitable for a forested wetland, but may be more appropriate for an emergent wetland.

Because wetlands are difficult to design more research is needed to create better models to ensure wetland success. Wetlands are dynamic systems, so to avoid failure the lifetime of a wetland should be considered in the initial design. Cole and Brooks (2000) even suggested allowing drier periods within constructed wetlands, so that the hydroperiod of mitigated wetlands matches that observed in reference wetlands more closely. Some of the changes that can occur in a wetland are sediment and peat build up and vegetation succession (Garbisch, 2002). These factors can alter wetland hydrology and can lead to failure if not considered thoroughly.

Wetland Hydrology

Wetland hydrology can be one of the most complicated elements of a wetland to recreate. While conceptual models have been created to simply explain wetland hydrology, actually quantifying each element can be difficult. Equation 1 illustrates one such water balance as follows:

$$\frac{\Delta V}{\Delta t} = P_n + S_i + G_i - ET - S_o - G_o \pm T \quad (1)$$

where $\frac{\Delta V}{\Delta t}$ is the change in volume of water storage in wetland per unit time, P_n is net precipitation, S_i is surface inflow, including flooding streams, G_i is groundwater inflow, ET is evapotranspiration, S_o is surface outflow, G_o is groundwater outflow, and T is tidal inflow (+) or outflow (-) (Mitsch and Gosselink, 2000).

The precipitation, surface inflow, and groundwater inflow and outflow are functions of the local climate, watershed, and geology; therefore, the main control the wetland designer has on the water budget is the wetland topography, vegetation, and outlet structure. For design, surface flows are typically routed through the wetland using level pool routing and assuming outflows are controlled by the outlet structure. However, dense emergent wetland vegetation provides extensive flow resistance, altering the water surface slope in the wetland. Four different flow types result from the inflows and the impact of frictional forces on surface flow in wetlands (Bedient and Huber, 1992): steady uniform, diffusion, steady nonuniform, and unsteady nonuniform. In steady uniform flow the bed slope and the friction slope are equal.

Because of the physical complexity of wetlands, the effects of momentum must also be assumed to be more complex. Momentum is the most complex for the unsteady,

nonuniform flow type, and the depth-averaged, one-dimensional calculation is as follows (Bedient and Huber, 1992):

$$S_f = S_o - \frac{\partial y}{\partial x} - \left(\frac{v}{g}\right)\frac{\partial v}{\partial x} - \left(\frac{1}{g}\right)\frac{\partial v}{\partial t} \quad (2)$$

where S_f is the friction slope, S_o is the bed slope, v is velocity, and g is gravity. The last two terms in the equation represent the longitudinal velocity gradient and the time rate of change of velocity, respectively. Because wetland flow is steady and typically unchanging over a long period of time, the time rate of change for velocity term can be removed. The resulting momentum equation is that of the steady nonuniform flow type.

Simplifying the momentum equation gives insight to what flow type can be assumed for wetland conditions. While steady nonuniform flow is valid for some conditions, the momentum equation can be further simplified by removing the longitudinal velocity gradient term, assuming that velocity is constant throughout the entire wetland. This simplification results in the momentum equation for the diffusion model, as follows:

$$S_f = S_o - \frac{\partial y}{\partial x} \quad (3)$$

Further simplifying the momentum equation leads to the assumptions for Manning's equation and, as previously stated, would be too simple for wetland flow conditions. Steady non-uniform flow and the diffusion model balance simplicity while still considering complexity of wetland flows.

Hydraulic Resistance due to Vegetation

Flow conditions in the wetland affect the vegetation as described below for increasing flow depth and velocity (Piercy, 2010):

1. Lowest power; vegetation stationary; no deflection;
2. Vegetation stationary with stems and leaves oriented downstream;
3. Stiff vertical stems vibrate; oblique or elongated horizontal stems movement;
4. Stiff stems deflected; submerged leaves oriented with flow; loss of dead parts of vegetation;
5. Stiff stems becoming prone or compacted, surface leaves submerged; and,
6. Highest power; severe damage or loss of parts or entire plant.

Because of the variety of ways that vegetation and water can interact, it is essential to understand how and why different vegetation types respond to each scenario. In a laboratory flume study, Sand-Jensen (2003) used real and constructed plants with varying frontal areas and flexibility to determine how the plant characteristics affected the vegetative drag in a flume setting. Study results indicated drag increased with plant frontal area but, as velocities increased, the plants would bend and create less drag. The plants would bend up to a threshold velocity (typically 50 cm/s for each plant) where the force bending the plants could not completely counteract the lift on the stems due to the water. Also, the variability in drag coefficient increased with increasing plant flexibility.

Not only can the individual plant properties affect water flow, but so can a plant community as a whole. Bennett and Simon (2004) used wooden dowels to simulate a plant community, and found that as the density of the plant community increases, water depth increases, and velocities decrease. Also, turbulent activity, such as surface waves, flow separation, and vertical structures, increase and become more apparent within the vegetated flow area as flow rates increase. Nepf (1999) also used wooden dowels to simulate vegetation and found contradicting results, including that as plant density

increased mean flow velocity decreased, but that increased density also led to a decrease in turbulence intensity.

Liu et al. (2008) found that velocities within simulated emergent vegetation were dependent on plant density and location. Plexiglas rods were used in this study to simulate vegetation. As the density of rods increased, the velocities changed more with location, while at the lower density configurations velocity remained fairly constant among different locations. The velocity profiles were also affected by the presence of the dowels. Directly behind the dowels the streamwise velocities were lowest with negative spikes. The streamwise velocities increased further downstream from the dowel, but the velocity profiles remained uniform with distance from the bed at each location. For submerged dowel cases, velocity profiles remained uniform until an inflection point occurred around the top of the dowel. The location of the inflection point depended on flow rate and vegetation density.

Jarvela (2002) used a variety of vegetation planted in a flume. Combinations of sedges, grasses, and willows were used to simulate wetland vegetation. When the density of plants was increased, the friction factor increased. Friction factor also increased linearly with depth until the plants were submerged. Once the plants were submerged the friction factor did not keep increasing at the same rate. Even though some of the vegetation used in this study had a tufted growth form, the length scale used was stem diameter.

Typically, vegetation impacts on surface flows are calculated using stem diameter as the representative length scale; however, wetland vegetation can exhibit a tuft or clump growth pattern. *Juncus effusus,* a common emergent wetland plant, grows in a

densely tufted pattern (Strausbaugh and Core, 1978). As a result of this growth pattern, water moves predominately between the clumps instead through individual stems.

Predicting Vegetative Resistance

Vegetation can contribute to the hydraulic resistance in a wetland in four ways: (1) form drag due to the difference in hydrodynamic pressure around an object or stem; (2) skin drag due to shear stresses from contact of flow with surfaces; (3) wave drag due to the deformation of the water surface where stems penetrate; and, (4) energy losses from turbulence and viscosity (Roig, 1994). Because there are a variety of factors, drag can be difficult to determine for all vegetation types.

Quantifying the impact of vegetation on flow resistance can be done with friction factor or drag coefficient. Several studies focus on the relationship of drag and vegetation characteristics, but these relationships are not comparable unless the reference areas are computed similarly (Järvelä, 2004). The friction factor is a dimensionless measure of flow resistance, but is highly dependent on water surface slope and velocity, which can cause lead to errors in predicting vegetation effects (Kadlec, 1990). Friction factor was first used to describe resistance in pipe flow, and was adapted for open channel flow (Brown, 2002). Because open channels do not have a uniform radius, hydraulic radius (Equation 4) has been used as a replacement length scale.

$$R_H = \frac{A}{P_w} \tag{4}$$

where R_h is the hydraulic radius, A is the area, and P_w is the wetted perimeter. If obstructions, such as vegetation, influence the flow area significantly, the hydraulic radius can be difficult to quantify.

Another common method used for quantifying hydraulic resistance is Manning's equation, as follows:

$$V = \frac{K}{n} R^{2/3} S^{1/2} \tag{5}$$

where V is velocity (m/s or ft/s), K is a conversion constant for English units, n is Manning's roughness coefficient, R is hydraulic radius (m or ft), and S is slope. The underlying assumptions of Manning's equation are that the soil surface provides the flow resistance and the flow is steady and uniform. Because, wetland flow resistance is primarily controlled by vegetative drag, wetland hydraulic resistance should not be modeled with Manning's equation (Kadlec, 1990).

As discussed previously, wetland hydraulic resistance can be difficult to quantify due to the variety and complexity of vegetation within wetlands. Also, because each study cites different length scales, such as water depth or diameter, comparing studies can be difficult. To unite several studies, Cheng and Nguyen (2011) developed a length scale similar to an open channel flow hydraulic radius, that compensates for emergent vegetation. The proposed hydraulic radius considers channel geometry and the size and arrangement of vegetation, as shown below:

$$r_v = \frac{(1-\lambda)BHL}{NDH} = \left(\frac{\pi}{4}\right)\frac{1-\lambda}{\lambda} D \tag{6}$$

where r_v is the vegetated hydraulic radius, B is channel width, H is water depth, L is channel length, N is the number of stems, D is stem diameter, and λ is the fraction of vegetated occupied bed area. Using r_v as the length scale for determining friction factor modifies the hydraulic radius based on vegetation. The developed friction factor equation is as follows:

$$f = \frac{8 g r_v S}{V_v^2} \tag{7}$$

where f is the friction factor, g is gravity, r_v is the hydraulic radius of the vegetation, S is the energy slope, and V_v is the pore velocity around the vegetation. The length scale was also used to calculate a Reynolds number. The r_v length scale allowed comparison of different studies with different methods on the same basis.

In a similar study, Piercy (2010) summarized how drag can be calculated for vegetation, and found the parameters that most influence vegetation drag. These parameters were the plant frontal area, height, volume, and flexural rigidity, as well as fluid viscosity. Using a series of flume studies with real vegetation, the following equation was developed to determine vegetative friction factor based on plant and flow characteristics:

$$f = 10^{a}(maa \cdot d)^{b} Re_{stem}^{c} \quad (8)$$

where f is friction factor, maa is momentum absorbing area, d is stem diameter, Re is the Reynolds number with a stem length scale, and a, b. and c are specific coefficients for each plant type. Because real vegetation was used in this study, the conditions are more representative of actual wetland vegetation. Momentum absorbing area is the amount of frontal area per unit volume.

Summary

Wetlands and their conservation are important. Designing wetlands to include vegetation impacts on wetland hydrology would improve the success of constructed wetlands. While vegetation clearly impacts surface water flow, predicting vegetation resistance to flow can be difficult due to the diversity of vegetation. Several wetland studies have simulated wetland vegetation using wooden dowels. These studies related measured velocities and water surface slopes to vegetation properties. However, there is

no known research evaluating the effects of vegetation clumping on flow through emergent wetlands.

Chapter 3. Methods

Field Methods

To address the research objectives, a flume study was conducted with actual wetland plants. To inform the flume study, two wetlands were sampled in the Piedmont region of Virginia to determine representative emergent vegetation. Seven mitigation wetlands were toured and two wetlands that were most representative of the area and spanned a range of wetland age were selected for vegetation sampling: Bull Run (established in 2003; 38.858929°, -77.554770°) and Julie Metz (established in 1995; 38.605876°, -77.279683°). Figure 1 shows the location of each of the sampled mitigation sites.

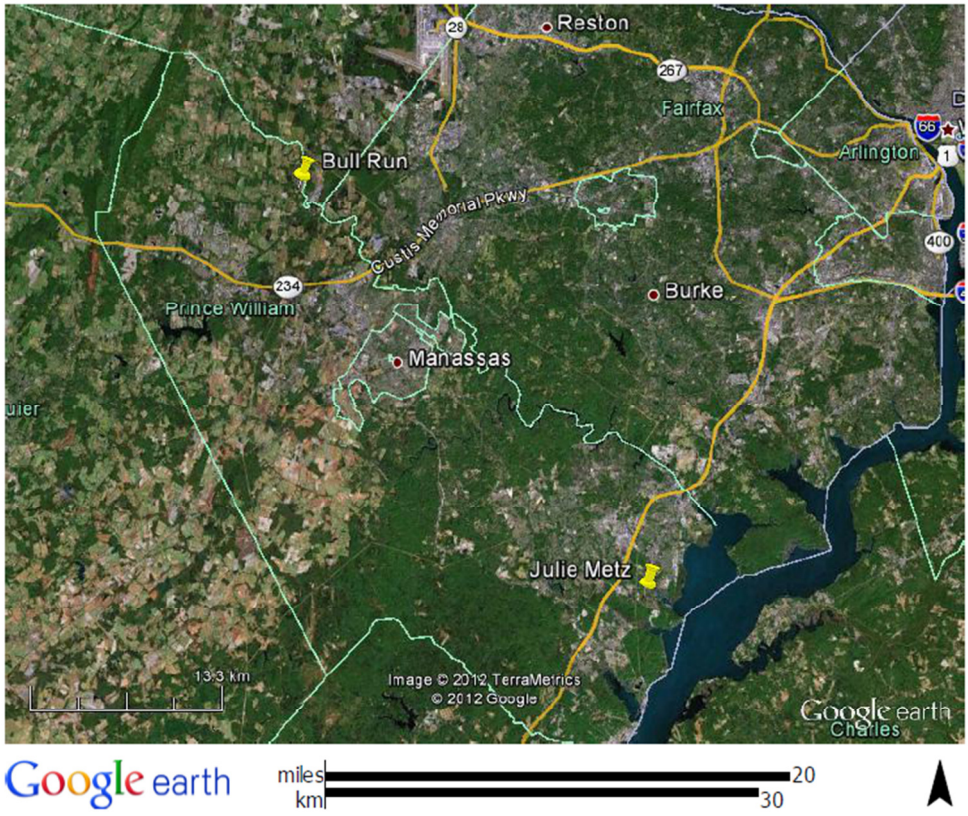

Figure 1. Location of Bull Run and Julie Metz mitigation sites used for quantifying Virginia Peidmont vegetation

Soft Rush (*Juncus effusus*) was prevalent at each site and was chosen as the vegetation for the study. While sampling, other species with similar growth forms to *Juncus effusus* were observed, but few broadleaf species were present. Small trees were present in the wetlands, but they had small diameter boles, and were widely spaced. The leaves on the trees were also well above expected water levels, so the effect of woody vegetation on shallow wetland flows was considered negligible. The age of the wetland impacted the density and size of the clumps. Figure 2 compares herbaceous vegetation growth at Bull Run and Julie Metz mitigation sites.

a) 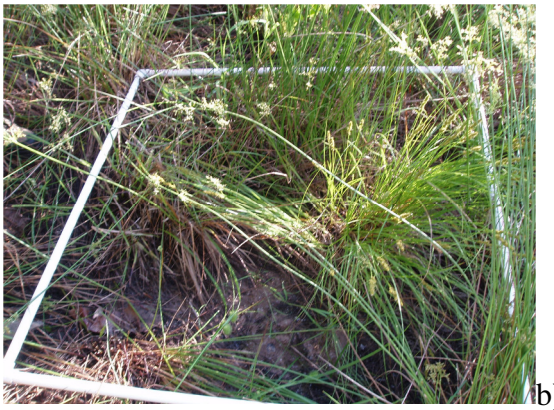 b) 

Figure 2. a) Younger wetland with dense, clumping vegetation; b) Older wetland with sparse vegetation

At each site three randomly selected 1-m quadrats were sampled. All vegetation within each quadrat was cut at ground level. Clump diameter was determined by measuring the greatest and smallest width and taking the geometric mean. Additionally, at each wetland plant diameter and location were identified in a 6 m by 1 m plot to determine average plant spacing.

Flume Methods

To construct the flume model, entire clumps of *Juncus effusus* were harvested from the floodplain wetlands along Stroubles Creek in Blacksburg, Virginia, USA in August 2011. The harvested clumps included the entire plant with the root mass and the accompanying soil. The plants were then formed into uniform clump diameters, consistent with the clumps in the sampled mitigation sites. The plants were then placed in a staggered pattern in a 6 m x 1 m x 0.4 m recirculating hydraulic flume (Engineering Laboratory Design, Inc., Minneapolis, MN, USA), with the test section located between 2.5 and 4.0 m longitudinally. The plants had uniform lateral and longitudinal spacing of 25 and 20 cm, on center. Plant placement began at the very edge of the flume to avoid flow short circuiting along the flume walls. Garden Pro Top soil (Garden Pro, Milford, DE, USA), a mineral top soil enhanced with organic compost and aged pine bark fines, was used as the bed to produce a realistic bed roughness and to allow the plants to root and continue to grow.. Once planted, the flume was filled and drained three times to settle the soil and to remove loose debris. Images of the flume set up are in Figure 3.

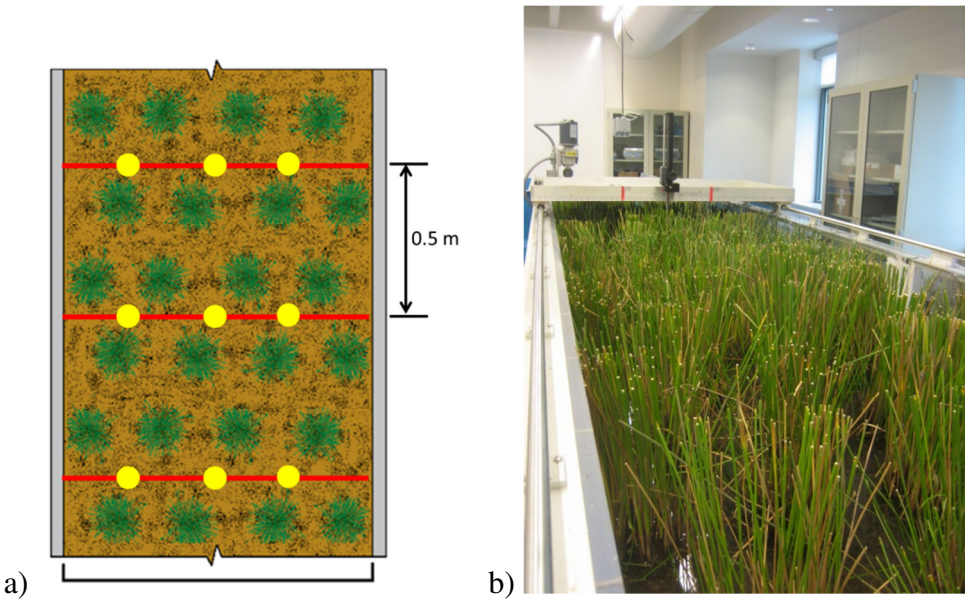

a) b)

c) 

Figure 3. Images of flume set up a) overhead view of flume set up (not to scale) where the yellow dots are water surface level measuring locations, b) actual view of flume with gage set up, c) view of a cross section in the initial flume set up (12 cm diameter, 25 cm spacing)

The plants were cut to uniform diameters of 12 cm, using 12 cm diameter tubes, and spaced at 25 cm, on center, in the flume. The plant spacing was then decreased to 20 cm. Once the tests with the 12 cm diameter clumps were complete the clump diameters were trimmed to 8 cm using 8 cm tubes. The trimmed stems were collected for analysis. The initial 8-cm plant spacing was 20 cm. Following completion of these tests, the spacing was then increased to 25 cm. The plants removed from the flume to increase plant spacing were analyzed to determine plant characteristics.

For each of the four flume setups (two clump diameters and two clump spacings), three different tailgate heights (5, 7.5, and 10 cm) and flows (3, 4, and 5 L/s) were examined (nine runs total for each setup) to document changes in water surface slope due to changes in clump size and spacing. The flume slope was held at a constant 0% slope

throughout the study; thus, measured water surface slopes were the result of flow resistance due to the channel boundary and the vegetation.

Once the flow in each run was fully developed, water surface measurements began. Flow was considered fully developed when the water surface elevations remained constant (± 0.3 mm) over a 30-min. period. Due to surface waves, water surface was determined as the average of the maximum and minimum water surface elevations . The minimum was determined by measuring the water height where the point gauge was constantly touching the water for at least one minute. The maximum was determined similarly, with the point gage continuously not touching the water for at least one minute. The minimum variability in water surface elevation allowed for a measurement to be considered stable was determined as the standard deviation of ten maximum and ten minimum water surface elevations at a single location. The water surface elevations were measured using a Series 570 Mitutoyo electronic height gage (Accuracy: 0.03 mm, Aurora, Illinois). Water surface measurements were taken at three positions laterally (40.5, 60.5, and 80.5 cm; pictured in Figure 3 as red dots) along eight cross sections longitudinally in the flume (1.0, 2.0, 2.5, 3.0, 3.5, 4.0, 4.5, and 5.0 m). At each measuring point minimum and maximum water surface levels were measured after zeroing the point gauge on the fiberglass surface of the flume beneath the soil. The soil surface was measured at the same locations before and after each run, to determine if soil erosion or deposition was occurring and to determine the flow depth at that location.

Actual water surface elevation at a given location was determined as the average of the maximum and minimum measured water surface elevations. Water surface slope was determined between consecutive cross sections for each of the three lateral

measurement locations. All of the slopes (three slopes each between three cross sections in the test section, for nine slopes total) were then averaged to get an average slope for each run. Head water and tail water effects between 2.5 and 4.0 meters longitudinally were minimal, as indicated in plots of water surface elevation over the flume length.

Water depth was calculated by subtracting the soil surface elevation from the water surface elevation. Then the depths within the test section were averaged and used in further calculations (n = 12).

To determine the bed roughness height, the soil surface was measured in detail at three cross sections after all the flume runs were completed. Measurements were taken every 5 cm or at slope breaks, depending on which was encountered first. The minimum height at each cross section was found, and was then subtracted from the rest of the measurements in that cross section to determine a bed roughness height. A histogram and cumulative distribution function were used to find the median roughness height (D_{50}). Data for determining the D_{50} can be found in Appendix A.

Velocity was measured using a Sontek 16 MHz Side-looking Micro-Acoustic Doppler Velocimeter (ADV; San Diego, California). Velocity profiles were measured at two flow rates (3 and 5 L/s) at a 7.5-cm tailgate height and a clump spacing and diameter of 25 cm and 8 cm, respectively. The ADV was aligned parallel to flow by measuring the distance from the flume wall to the probe, to ensure correct measurement of flow velocities in the streamwise, cross-channel, and vertical directions. Velocity profiles were measured at four locations relative to a representative vegetation clump to examine the change in the velocity profile between locations (Figure 4).

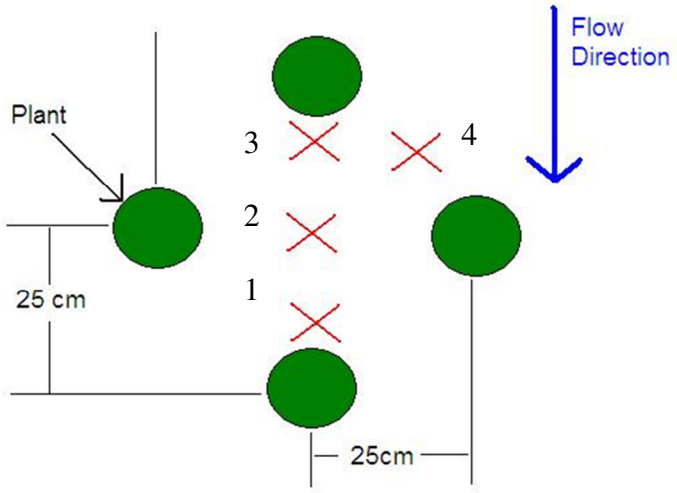

Figure 4. Locations of velocity profile measurement

At each profile measurement location, average velocities were measured for 1 min. at three distances above the soil surface (3.5, 4.0, and 4.5 cm) at a flow rate of 3 L/s and four distances above the soil surface (3.5, 4.0, 4.5, and 5 cm) at a flow rate of 5 L/s. Instantaneous velocity values with an average signal correlation value less than 70% or an average signal to noise ratio less than 15 were removed.

Plant Analysis Methods

After the flume runs were conducted the vegetation was removed and the amount of above-ground vegetation within the flume was quantified. Stems cut from the base of each clump were counted and then cut into 2.5-cm height increments (2.5, 5.0, 7.5, and 10.0 cm). The stems were then scanned with a Li-cor Model 3100 (Lincoln, Nebraska) area meter to measure stem frontal area per height increment. Stem frontal area was used to calculate average stem diameter at different water depths. The total frontal area was divided by the number of stems to find an average stem frontal area. The average stem

frontal area was then divided by 2.5 cm to find an average stem diameter at each height increment.

The clump and stem density and porosity were determined by calculating the number of clumps per square meter for each plant spacing. The average number of stems per clump was then used with clump density to find the average stem density at each plant spacing and clump diameter. Once stem and clump densities were determined, the known diameters of the stems and clumps were used to find the plant occupied bed area per unit of total bed area.

Clump basal heights were measured after the stems were cut from the plant. Figure 5 shows where the stems were cut and where the top of the clump base was measured.

Figure 5. Line where vegetation was cut to distinguish between the effective clump and the rest of the plant

The clump basal area was identified as the region above the soil surface where the stems formed a compact mass that did not allow water to flow through the clump.

Determination of Model Parameters

Parameters considered for inclusion in the friction factor model were determined as described below.

Momentum absorbing area is the frontal area of the plants per unit volume and was calculated using Equation 9

$$MAA = \frac{NDH}{BLH} = \rho_{plants} D \tag{9}$$

where MAA is the momentum absorbing area, N is number of stems, D is stem diameter, H is water depth, B is the flume width, L is the flume length, and ρ_{plants} is the number of plants per square meter. Average pore velocity (Cheng and Nguyen, 2011) of the flow was calculated as follows using the plant occupied bed area, flume dimensions, and the flow rate (Equation 10):

$$V = \frac{Q}{BH(1-P)} \tag{10}$$

where V is the average pore velocity, Q is the discharge, B is the width of the flume, H is the water depth, and P is the plant occupied bed area. An alternate length scale suggested by Cheng and Nguyen (2011) was also calculated using Equation 11:

$$r_v = \frac{\pi}{4}\frac{1-P}{P} D \tag{11}$$

where r_v is the vegetated hydraulic radius, P is the fraction of occupied vegetated bed area, and D is the diameter (stem or clump). Friction factor was calculated using a Colebrook-type resistance relation (Cheng and Nguyen, 2011) (Equation 12):

$$f = \frac{8 g r_v S}{V^2} \tag{12}$$

where f is friction factor, g is gravity, r_v is vegetative hydraulic radius, S is water surface slope, and V is pore velocity through the vegetation.

Buckingham Pi

Buckingham Pi analysis (Sabersky, 1999) was conducted to develop non-dimensional parameters that describe the influence surface water flow through emergent vegetation. Several plant and flow parameters characterize the effects of vegetative hydraulic resistance, as summarized in Piercy (2010). Based on the Piercy (2010) final regression model, nine parameters were selected for the dimensional analysis. Table 1 summarizes the characteristics chosen and the results of the Buckingham Pi analysis.

Table 1. Parameters and results from Buckingham Pi analysis describing the impacts of vegetation on flow resistance

Parameters	D*, H, MAA, V, S, ρ, μ, P, g
π Terms	f, S, P, MAA·D, D/H, Re, Fr

* D is stem or clump diameter, H is water depth, MAA is momentum absorbing area, V is the pore velocity, S is water surface slope, ρ is water density, μ is water viscosity, P is plant occupied bed area, and g is gravity

The Reynolds and Froude numbers were also a result of the analysis.

As discussed in Chapter 2, there is some debate among researchers regarding the best representative length scale to use in determining Reynolds number in emergent wetland flows. In Cheng and Nguyen (2011) the vegetative hydraulic radius (Equation 8) was used, so three Reynolds length scales were considered for further analysis: stem or clump diameter and vegetative hydraulic radius. Because both stem diameter and clump diameter were considered for further analysis, two sets of non-dimensional parameters were calculated, one using stem diameter and the other using clump diameter.

Sidewall and Bed Corrections

Bed and sidewall corrections were made to ensure the friction factor only reflected the vegetative drag. Methods from Cheng and Nguyen (2011) were used to remove the bed and sidewall influences from the friction factor calculated from the measured water surface slopes.

To calculate a corrected vegetated friction factor, a modified hydraulic radius was calculated. The equation proposed by Cheng and Nguyen (2011) is as follows:

$$r_{vm} = r_v \left[1 - \left(\frac{f_w}{0.5B(1-P)} + \frac{f_b}{h}\right)\frac{r}{f}\right] \quad (13)$$

where r_{vm} is the modified vegetated hydraullic radius, r_v is the raw hydraulic radius (Equation 8), f_w is the friction due to the wall, f_b is friciton due to the bed, h is water depth, B is bed width, r is hydraulic radius of the flume, and f is uncorrected friction factor. Iteration of the Colebrook equation must typically be conducted to find f_w and f_b; however, the following explicit equation was proposed by Cheng and Nguyen (2011):

$$f_w^{\alpha} = f_{wS}^{\alpha} + f_{wR}^{\alpha} \quad (14)$$

where

$$f_{wS} = 31\left[ln\left(1.3\frac{Re}{f}\right)\right]^{-2.7} \quad (15)$$

$$f_{wR} = 11.7\left[ln\left(7.6\frac{4r}{fk_{sW}}\right)\right]^{-2.5} \quad (16)$$

$$\alpha = 2\left(\frac{4r}{fk_{sW}}\right)^{0.1} \quad (14)$$

While equations 11-14 are shown for f_w, similar calculations can be made for f_b. The Reynolds number length scale is channel hydraulic radius, r, f is the friction factor (Equation 12), and k_s is the roughness height of either the wall or bed. The D_{50} calculated

from the three cross sections was used for the bed roughness and an assumed value of 0.0001 meters was used for the acrylic flume wall roughness. The modified vegetative friction factor was used in the regression analysis. All calculated values are in Appendix B.

Prediction equations were also developed using friction factors that incorporated vegetation and bed effects for use in wetland modeling. The prediction equation results for friction factors containing both vegetation and bed are reported in Appendix D. The regression techniques used are as follows.

Statistical Methods

Using the calculated non-dimensional terms, a regression analysis was conducted in MINITAB 16 (Minitab Inc., State College, PA, USA) statistical software to develop equations to predict the friction factor based on wetland vegetation properties. Using Variance Inflation Factors (VIFs) co-linearity among the terms was determined. A VIF greater than a value of 10 indicated the parameter was correlated with another parameter. When parameters were highly correlated, separate regression analyses were conducted. Next, the best subsets of the non-dimensional parameters were found based on adjusted R-squared, Mallows Cp, and stepwise regression. Mallows Cp compares the precision and bias of a model with all considered predictors to create model subsets. Mallows Cp helps find a balance in precision and bias. As Mallows Cp approaches the number of regressors the model performance increases. Adjusted R^2 is used for comparing the explanatory power of predictors. The value of Adjusted R^2 will only increase if the added predictor increases the model performance more than chance. The adjusted R^2 value is

different from the standard R^2 because standard R^2 will always increase when more predictors are added to the model.

Once the best subsets for the stem and clump parameters were found, three methods were used to find leverage points and outliers for each model: hii, DFITS, and Cook's D. Each method assesses how the model would change if an observation were removed from the dataset. The number of leverage points and the Press statistic for each model were then compared, and the subsets with the fewest leverage points and lowest Press statistic were considered the best models. PRESS statistic assesses the predictive ability of the model with smaller PRESS statistics indicating a stronger predictive ability of the model.

Chapter 4. Results and Discussion

The emergent *Juncus effsus* had a significant impact on flow, with flow characteristics varying with tailgate height and flow rate. The highest flow rates had the most turbulent conditions: the stems were observed to vibrate and eddies formed behind the plant clumps. For the two lower tailgate heights, small surface waves were visible, whereas water surface oscillation was minimal to nonexistent for the highest tailgate height.

Plant Analysis Results

As described in Chapter 3, plant stem diameter and number were measured to derive vegetation parameters (Table 3). The bed area occupied by plant stems, P_{stem}, ranged from 0.007 to 0.018, while P_{clump} ranged from 0.07 to 0.25. Because of space between stems within the clumps, the stem and clump P differed by an order of magnitude. The average stem diameter was 0.39 cm and was constant with distance from the bed over the lower 10 cm. These values are consistent with previous studies of wetland vegetation summarized by Cheng and Nguyen (2011). Reported stem diameters ranged from 0.3 to 0.8 cm, while values of P varied from 0.003 to 0.250, which are comparable to the plants and planting density in this study. The P of the clumps is similar to the higher values examined by Cheng and Nguyen (2011). Table 1 shows further results from the plant analysis.

Table 2. Plant analysis results

		Spacing (cm)	Clump Diameter (cm) 12	8
Avg. Stems per Clump		-	69	44
Clumps per m^2		20	23	-
		25	15	-
Stems per m^2		20	1549	985
		25	1032	657
P	Clumps	20	0.25	0.11
		25	0.17	0.08
	Stems	20	0.02	0.01
		25	0.01	0.01

Flume Observations

As the fraction of plant occupied bed area decreased slopes also decreased and became indistinguishable at the lowest flow rates and highest tail gate heights. The water surface slopes ranged from 0.001 to 0.008 over the entire study. Table 2 shows the values of slope and depth for each run of the flume.

These slopes are similar to energy slopes found by Jarvela (2002) of 0.0001 to 0.0127 for tufted sedges and willows in a flume study. For a plant spacing and diameter of 20 and 8 cm, respectively, slopes became immeasurable for flow rates of 3 and 4 L/s at the 7.5-cm tailgate height. When spacing was increased to 25 cm and the plant diameter was maintained at 8 cm slope was not measurable at the 7.5-cm tailgate height for any of the three flow rates. Slopes were also not measurable for flow rates at 3 and 4 L/s with a tailgate height of 5 cm.

Table 3. Depth and slope measurements for each flume run

Flow Rate (L/s)	Clump Spacing (cm)	Clump Diameter (cm)	Tailgate Height (cm)	Depth (mm)	Average Slope ± Std Dev
3	25	12	2.5	40.67	0.0055 ±0.0020
4				50.89	0.0070 ±0.0023
5				58.32	0.0052 ±0.0028
3			7.5	73.19	0.0012 ±0.0008
4				76.91	0.0018 ±0.0007
5				83.69	0.0028 ±0.0009
3			5	50.63	0.0019 ±0.0005
4				66.80	0.0024 ±0.0006
5				72.34	0.0035 ±0.0006
3	20		7.5	77.16	0.0012 ±0.0009
4				81.86	0.0019 ±0.0009
5				88.23	0.0032 ±0.0008
3			5	53.96	0.0024 ±0.0009
4				66.46	0.0045 ±0.0011
5				75.22	0.0057 ±0.0011
3			2.5	50.86	0.0055 ±0.0003
4				61.28	0.0064 ±0.0001
5				69.31	0.0077 ±0.0022
3	20	8	2.5	45.70	0.0044 ±0.0005
4				60.42	0.0057 ±0.0004
5				67.02	0.0062 ±0.0005
3			5	54.77	0.0028 ±0.0004
4				64.56	0.0042 ±0.0004
5				71.81	0.0051 ±0.0005
5			7.5	86.64	0.0021 ±0.0005
4	25		5	60.93	0.0019 ±0.0007
5				65.44	0.0028 ±0.0008
3			2.5	39.43	0.0028 ±0.0009
4				48.51	0.0038 ±0.0013
5				56.13	0.0048 ±0.0007

Changes in bed surface elevation during an individual flume run ranged from -16.23 mm at 4.5 m longitudinally to +13.82 mm at 5 m longitudinally. The maximum amount of erosion occurred after plants were moved. No pattern in the bed changes were discernible, as the changes in bed elevations at each measurement point were not

consistent along or across the flume. The lack of an erosion and deposition pattern could be a result of differences in the bed density. Erosion and deposition at each water surface measurement point changed from one run to the other; these changes and the associated sediment transport could contribute to some of the error in the results. Because the soil surface changed every time the plants were reconfigured a change in bed surface cannot be calculated over the entire study. At the end of the study bed height measurements were taken at three different cross sections as described in Chapter 3 to find a mean roughness height. The D_{50} from the three cross sections was 9 mm.

As described in Chapter 3, plants were trimmed above the clump basal layer. When the stems were trimmed from the plant, only the dense basal layer was left. Figure 6 shows the difference between the full and trimmed plants.

Figure 6. Plants were trimmed, so that clump heights could be measured.

The average height of the clump basal layer was 114 mm, as measured from the Plexiglas surface of the flume. Depending on soil depth around each clump, this represented a protrusion height of approximately 56 mm above the soil surface. When water depth was above the clump basal layer, water moved between the individual stems in a clump. When water depth was lower than the clump basal layer, flow was primarily between the clumps. Water depth exceeded the average clump basal layer height during 40% of the flume runs.

Velocity Profiles

To examine differences in flow velocities in relation to the clumps, velocity profiles were measured at four locations. The velocity profiles (Figures 7 and 8) illustrate that the water flowed around the clumps and created eddies behind the clumps. Because the water depth was greater during the 5 L/s flow rate, four velocity measurements were taken at each of the four points, while only three measurements were taken during the 3 L/s flow rate. At each location, point velocity measurements were taken every 0.5 cm from the bottom of the bed to the water surface. At the lowest point measured the ADV was touching the bed surface; however, because the ADV probe was side-looking, the lowest velocity measurement was 3.5 cm above the bed. Figures 7 and 8 show the results of the velocity profile measurements of the 3 L/s and 5 L/s flow rates, respectively.

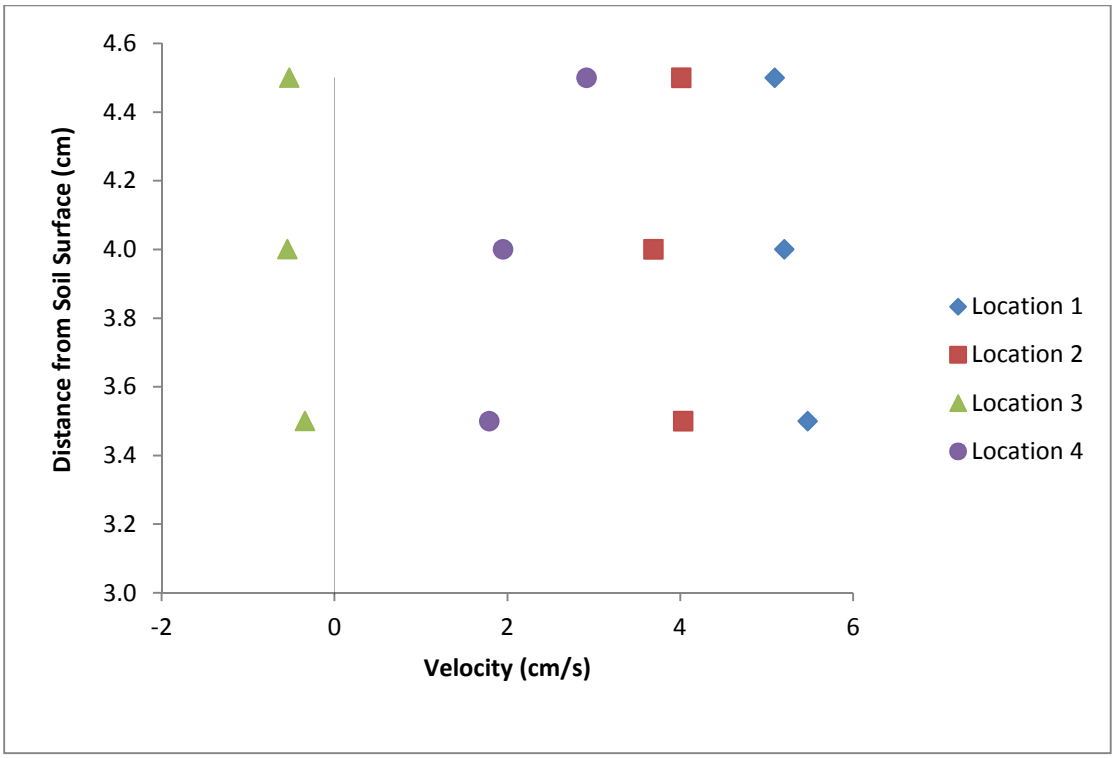

Figure 7. Velocity profiles for 3 L/s at 7.5 cm tailgate height where Location 1 is directly in front of the plant, Location 2 is in the middle of four plants, Location 3 is directly behind a plant, and Location 4 is diagonally between two plants.

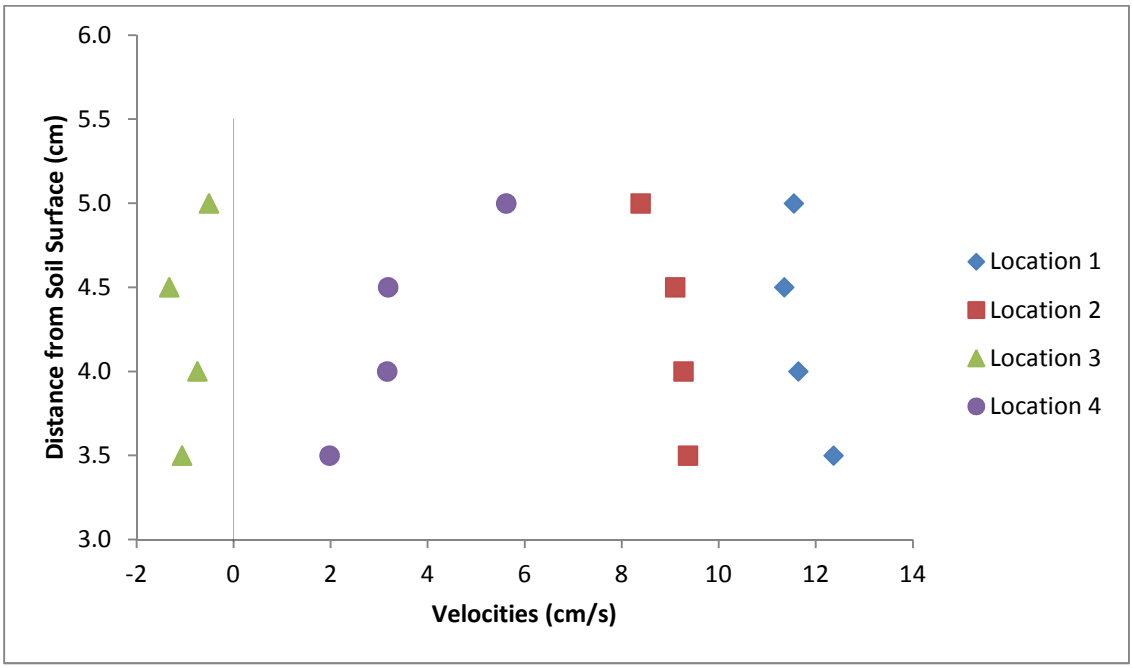

Figure 8. Velocity profiles for 5 L/s at 7.5 cm tailgate height where Location 1 is directly in front of the plant, Location 2 is directly in the middle of four plants, Location 3 is directly behind a plant, and Location 4 is diagonally between two plants.

Figures 7 and 8 show that the velocities varied depending on the location relative to the plants. At locations 1, 2, and 3 the velocity profiles were relatively uniform, with only the magnitudes varying. The negative velocities directly behind the clumps indicate the presence of eddies. Downstream from the clumps, the velocities increase but remain generally uniform with depth. The maximum velocities occur directly in front of the clump. The velocity profiles at Location 4, which is diagonally between two plants, is more typical of velocity profiles in unvegetated flows, where bed roughness is the main influence on the flow. The velocities at the bottom are lower and increase with increasing proximity to the free surface where there is minimal influence from the bed roughness. Figure 9 shows sediment deposition behind the clumps in response to the negative velocities.

Figure 9. Deposited sediment behind plants

The sediment deposited behind the clumps is evidence that the plant clumps did influence the flow. The deposited sediment also confirms the velocity profile measurements. In a study of Plexiglass dowels, Liu et al. (2008) also observed that velocities were dramatically lower directly behind the simulated vegetation; negative instantaneous velocities occurred even though the mean velocity was positive. Also, at locations further downstream of the dowel the velocities increased.

Data Analysis Results

As described in Chapter 3, ten nondimensional parameters were developed to describe flow through clumped wetland vegetation. All Buckingham Pi parameters described in Chapter 3 were calculated from measured water surface slope, bed elevation, vegetated occupied area, and flow rate. Because clump diameter was evaluated as a length scale, as well as stem diameter, each calculation was completed for both P_{clump} and P_{stem}. Additionally, two Reynolds numbers were calculated for each set of clump and stem parameters, because the Cheng and Nguyen (2011) length scale, r_v, was also considered as a length scale for Reynolds number (Figure 10). Tables 4 and 5 show the parameters calculated from the Buckingham Pi analysis.

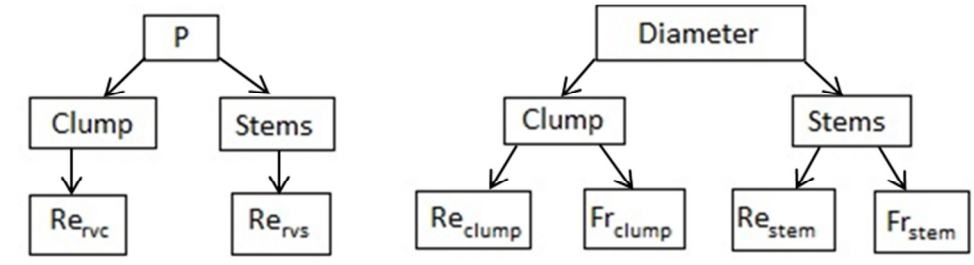

Figure 10. Flowchart to visually describe and explain the non-dimensional parameters and length scales used in their calculation

Table 4. Clump-based parameters

P*	V_v (cm/s)	r_v (m)	f_v	Re_{rv}	D/H	MAA (m^{-1})	MAA*D	Fr	Re_{clump}	Re_{depth}
0.17	8.9	0.46	25	41000	3.0	1.8	0.22	0.03	10700	3600
	9.5	0.46	28	44000	2.4	1.8	0.22	0.03	11000	4800
	10.3	0.46	18	48000	2.1	1.8	0.22	0.03	12000	6000
	4.9	0.46	18	23000	1.6	1.8	0.22	0.01	5900	3600
	6.3	0.46	17	29000	1.6	1.8	0.22	0.02	7500	4800
	7.2	0.46	20	33000	1.4	1.8	0.22	0.02	8600	6000
	7.1	0.46	14	33000	2.4	1.8	0.22	0.02	8600	3600
	7.2	0.46	17	33000	1.8	1.8	0.22	0.02	8700	4800
	8.3	0.46	18	38000	1.7	1.8	0.22	0.02	9900	6000
0.25	5.2	0.28	10	14000	1.6	2.7	0.32	0.02	6300	4000
	6.6	0.28	10	18000	1.5	2.7	0.32	0.02	7900	5400
	7.6	0.28	12	21000	1.4	2.7	0.32	0.02	9100	6700
	7.5	0.28	9	21000	2.2	2.7	0.32	0.02	8900	4000
	8.1	0.28	15	22000	1.8	2.7	0.32	0.02	9700	5400
	8.9	0.28	16	25000	1.6	2.7	0.32	0.03	10000	6700
	7.9	0.28	19	22000	2.4	2.7	0.32	0.02	9500	4000
	8.8	0.28	18	24000	2.0	2.7	0.32	0.03	11000	5400
	9.7	0.28	18	27000	1.7	2.7	0.32	0.03	12000	6700
0.11	7.4	0.49	31	36000	1.8	1.8	0.14	0.03	5900	3400
	7.5	0.49	40	37000	1.3	1.8	0.14	0.03	5900	4500
	8.4	0.49	34	41000	1.2	1.8	0.14	0.03	6700	5600
	6.2	0.49	28	30000	1.5	1.8	0.14	0.02	4900	3400
	7.0	0.49	33	34000	1.2	1.8	0.14	0.03	5600	4500
	7.8	0.49	32	39000	1.1	1.8	0.14	0.03	6200	5600
	6.5	0.49	19	32000	0.9	1.8	0.14	0.02	5200	5600
0.08	7.1	0.77	23	55000	1.3	1.2	0.10	0.03	5700	4300
	8.3	0.77	25	64000	1.2	1.2	0.10	0.03	6600	5400
	8.2	0.77	25	63000	2.0	1.2	0.10	0.03	6600	3200
	8.9	0.77	29	69000	1.6	1.2	0.10	0.03	7100	4300
	9.6	0.77	32	74000	1.4	1.2	0.10	0.03	7700	5400

*D is stem or clump diameter, H is water depth, MAA is momentum absorbing area, V_v is the pore velocity, r_v is the vegetated hydraulis radius, P is plant occupied bed area, Fr if Froude number, f_v is the friction factor of the vegetation, Re_v is the Reynolds number where the length scale is r_v, and Re_{clump} is the Reynolds number found from the Buckingham Pi analysis (length scale is clump diameter)

Table 5. Stem-based parameters

P*	Avg. Pore Velocity (cm/s)	r_v (m)	f_v	Re_{rv}	D/H	MAA (m^{-1})	MAA*D	Fr	Re_{stem}	Re_{depth}
0.012	7.47	0.25	19	18000	0.10	4.0	0.016	0.12	290	3000
	7.96	0.25	21	19000	0.08	4.0	0.016	0.13	310	4100
	8.68	0.25	13	21000	0.07	4.0	0.016	0.14	340	5100
	4.15	0.25	14	10000	0.05	4.0	0.016	0.07	160	3000
	5.27	0.25	13	13000	0.05	4.0	0.016	0.09	210	4100
	6.05	0.25	15	15000	0.05	4.0	0.016	0.10	240	5100
	6.00	0.25	10	15000	0.08	4.0	0.016	0.10	230	3000
	6.06	0.25	12	15000	0.06	4.0	0.016	0.10	240	4100
	7.00	0.25	14	17000	0.05	4.0	0.016	0.11	270	5100
0.018	3.96	0.16	10	6400	0.05	6.0	0.024	0.06	150	3100
	4.98	0.16	10	8100	0.05	6.0	0.024	0.08	200	4100
	5.77	0.16	12	9400	0.04	6.0	0.024	0.09	230	5100
	5.66	0.16	9	9200	0.07	6.0	0.024	0.09	220	3100
	6.13	0.16	15	9900	0.06	6.0	0.024	0.10	240	4100
	6.77	0.16	16	11000	0.05	6.0	0.024	0.11	260	5100
	6.01	0.16	19	9800	0.08	6.0	0.024	0.10	230	3100
	6.65	0.16	18	11000	0.06	6.0	0.024	0.11	260	4100
	7.35	0.16	18	12000	0.06	6.0	0.024	0.12	290	5100
0.012	6.64	0.26	20	17000	0.09	2.7	0.011	0.11	260	3000
	6.70	0.26	26	17000	0.06	2.7	0.011	0.11	260	4000
	7.55	0.26	22	19000	0.06	2.7	0.011	0.12	290	5100
	5.54	0.26	18	14000	0.07	2.7	0.011	0.09	220	3000
	6.27	0.26	22	16000	0.06	2.7	0.011	0.10	250	4000
	7.05	0.26	21	18000	0.05	2.7	0.011	0.12	280	5100
	5.84	0.26	12	15000	0.05	2.7	0.011	0.10	230	5100
0.008	6.62	0.39	13	26000	0.06	1.8	0.007	0.11	260	4000
	7.70	0.39	14	29000	0.06	1.8	0.007	0.13	300	5000
	7.67	0.39	14	29000	0.10	1.8	0.007	0.13	300	3000
	8.31	0.39	17	32000	0.08	1.8	0.007	0.14	320	4000
	8.98	0.39	18	35000	0.07	1.8	0.007	0.15	350	5000

*D is stem or clump diameter, H is water depth, MAA is momentum absorbing area, V_v is the pore velocity, r_v is the vegetates hydraulis radius, P is plant occupied bed area, Fr if Froude number, f_v is the friction factor of the vegetation, Re_v is the Reynolds number where the length scale is r_v, and Re_{stem} is the Reynolds number found from the Buckingham Pi analysis (length scale is stem diameter)

Because of differences in the calculation of P (using clump diameter versus stem diameter) the friction factors, Reynolds numbers, and Froude numbers for the stems are much lower than those for the clumps.

Despite the differences in the fraction of plant occupied bed area, P, the calculated friction factors for each were very similar. Friction factors increased with decreasing depth. At larger depths, velocities were slower, so friction factor decreased. Figure 2 compares the friction factor of the clumps to that of the stems.

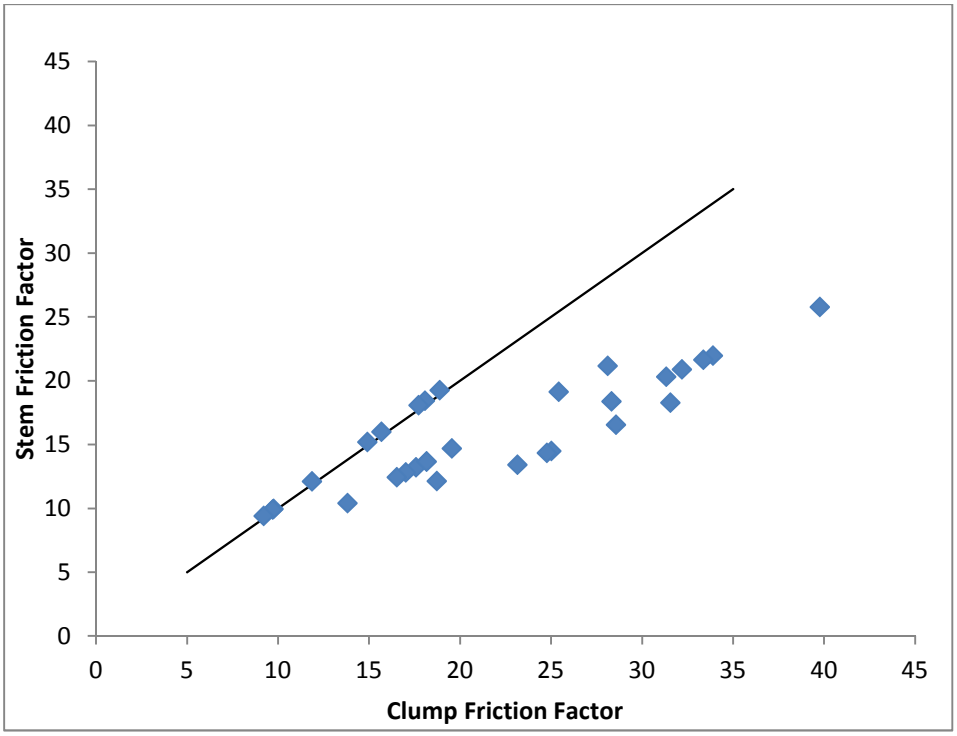

Figure 11. Comparison of stem and clump friction factors along with a 1:1 line

Comparing the data to a 1:1 line the stem friction factors are generally lower than the clump friction factors, particularly at the higher friction factors. The stem friction factors match the clump friction factors at low values where the vegetation density was greatest, but as the clump friction factors increase the differences between the clump and stems values also increases. The runs conducted at the highest P have matching clump and stem

friction factors, and fall on the 1:1 line in Figure 5. Because of differences in the fraction of plant occupied bed area, the vegetated hydraulic radius and pore velocity were different between the stem-based and clump-based parameters, resulting in differences in the friction factors except for the highest P cases.

Statistical Results

A regression analysis was conducted to develop a model for friction factor based on dimensionless vegetation parameters. The parameters calculated with stems were separated from the parameters calculated with the clumps during the analysis and the models found from each regression were compared. Minitab outputs can be found in Appendix C.

Clump Regression

The analysis showed that MAA and P were highly collinear, indicating they could be used interchangeably in the analysis. Because P is simpler to quantify, MAA was not used for further analysis. P can be measured in the field by nondestructive sampling. To calculate MAA plants must be cut and brought to the lab for measurement. Mallows Cp, adjusted R^2, and stepwise regression were used to find the best subsets, as shown in Table 6.

Table 6. Best model subsets of clump regression

Parameters*	Mallows Cp	Adjusted R^2	# of Leverage Points	Press Statistic	R^2
P, D/H	28.6	54.9	8	927	58.0
P, Re_{rv}	28.2	55.2	7	907	58.0
P, Re_{clump}	28.0	55.3	5	898	58.4
P, Re_v, Fr	3.7	77.1	4	489	79.0

* D is stem or clump diameter, H is water depth, P is plant occupied bed area, Fr if Froude number, Re_{rv} is the Reynolds number where the length scale is r_{vc}, and Re_{clump} is the Reynolds number found from the Buckingham Pi analysis (length scale is clump diameter)

Mallows Cp compares the precision and bias of a model with all considered predictors to model subsets and helps find a balance in the number of model predictors . As Mallows Cp approaches the number of regressors, the model performance increases. Adjusted R^2 is used for comparing the explanatory power of predictors. The value of Adjusted R^2 will only increase if the added predictor increases the model performance more than chance. The adjusted R^2 value is different from the standard R^2 because standard R^2 will always increase when more predictors are added to the model. Once the best subsets of the parameters were found, they were compared based on the R^2, Press statistic, and the number of leverage points. The PRESS statistic assesses the predictive ability of the model with smaller PRESS statistics indicating a stronger model predictive ability. Based on data presented in Table 4, the last two subsets (P, Re_{clump} and P, Re_{rv}, Fr) were the best models based on the clump data. The models for each are shown in equations 15 and 16,

$$f = 34.5 - (49.9 \times P) + (0.000312 \times Re_{clump}) \quad (15)$$

$$f = 28.5 - (133 \times P) - (0.000473 \times Re_{rv}) + (1284 \times Fr) \quad (16)$$

where f is friction factor, P is the fraction of plant occupied bed area, Re_{clump} is the Reynolds number found in the Buckingham Pi analysis, Re_{rv} is the Reynolds umber developed in Cheng and Nguyen (2011), and Fr is the Froude number. The models in this study show a decrease in friction factor with increasing P; P increases with depth, and when depth increases velocities decrease due to an increase in flow area, resulting in reduced friction losses. The greatest friction factors were at the lowest depths when velocities were highest.

Stem Regression

In the initial analysis, two sets of parameters were highly collinear: Froude number with the Re_{stem} and MAA with P. As stated above, P was used instead of MAA due to the simplicity in measurement. Stem Froude and Stem Reynolds numbers were highly collinear and interchangeable. The Stem Froude number was used to eliminate a Reynolds number from potential models. Mallows Cp, adjusted R^2, and stepwise regression were all used to find the best subsets. Table 5 shows the best subsets found.

Table 7. Best model subsets of stem regression

Parameters*	Mallows Cp	Adjusted R^2	# of Leverage Points	Press Statistic	R^2
Re_{rv}, Fr	30.3	19.5	9	348.9	25.1
P, Re_{rv}	21.2	32.9	5	296.9	37.5
P, Re_{rv}, Fr	4.5	59.2	5	192.9	63.5
P, Fr, D/H	19.2	36.6	5	302	43.2
P, Re_{rv}, D/H	20.0	35.4	7	310	42.1

* D is stem or clump diameter, H is water depth, P is plant occupied bed area, Fr if Froude number, and Re_{rv} is the Reynolds number where the length scale is r_{vs}

Once the best subsets of the parameters were found, they were compared based on their R^2, Press statistic, and the number of leverage points. Based on the data presented in Table 6, the models with five leverage points were considered the best models using the stem diameter as the representative length scale. The models developed based on the best subsets are shown in equations 17, 18 and 19.

$$f = 18.6 - (558 \times P) - (0.00076 \times Re_{Rv}) \quad (17)$$

$$f = 14.7 - (998 \times P) - (0.000691 \times Re_{Rv}) + (182 \times Fr) \quad (18)$$

$$f = 8.65 - (359 \times P) + (42.5 \times Fr) + (26.7 \times {}^{D}/_{H}) \quad (19)$$

where f is friction factor, P is the fraction of plant occupied bed area, Re_{rv} is the Reynolds number developed in Cheng and Nguyen (2011), Fr is the Froude number, and D/H is the

diameter to flow depth ratio. As with the clump-based length scale, P and friction factor are inversely related. When vegetation density increases, the available area for flow decreases, increasing flow depth and reducing velocity, which in turn reduces the friction factor. In a coupled laboratory and field study, Nepf (1999) found that as vegetation density increased, turbulence decreased due to a reduced mean velocity. In a study of real and constructed vegetation in a flume setting, Sand-Jensen (2003) also found that as the number of shoots and leaves increased, the drag coefficient decreased. Opposite results were reported by Jarvela (2002), who showed a positive relationship between vegetation density and friction factor. This difference is likely the due to the fact that Jarvela used depth as the length scale when calculating friction factor; increases in vegetation density resulted in an increase in depth and an increase in friction factor. Using r_v as the length scale, the amount of vegetation in the channel is in taken into consideration through the length scale. Thus, increases in vegetation density are indicated by a decrease in the length scale.

Basic Model

Because P was in every model, it was the most significant parameter of the study. A simple model based only on P was evaluated for clumps and stems (equations 20 and 21), to compare predictions based on a single parameter to the prior models.

$$f = 36.0197 - (88.9369 \times P_{clump}) \tag{20}$$

The model had an R^2 of 58 and a PRESS statistic of 853. These values show that this simple model predicts as well as model 1 (Equation 15) and not quite as well as model 2 (Equation 16).

For stems, a simple model was also found because P also was an important parameter in the stem-based models. The simple stem-based model is as follows:

$$f = 16.1 - (463 \times P_{stem}) \quad (21)$$

The model had an R^2 of 37 and a PRESS statistic of 284. The simple model for the stems does not predict quite as well as models 3, 4, and 5, (Equations 17, 18, and 19), as indicated by the low R^2, but the simplicity of the model is a benefit.

Comparing Models

The best models in each regression set had four or five leverage points and had R^2 values of 0.37 to 0.79. To visually compare the models, the predicted friction factor was plotted versus the calculated friction factor and compared to a 1:1 line. Figure 11 is a graph of the clump models and Figure 12 is a graph of the stem models.

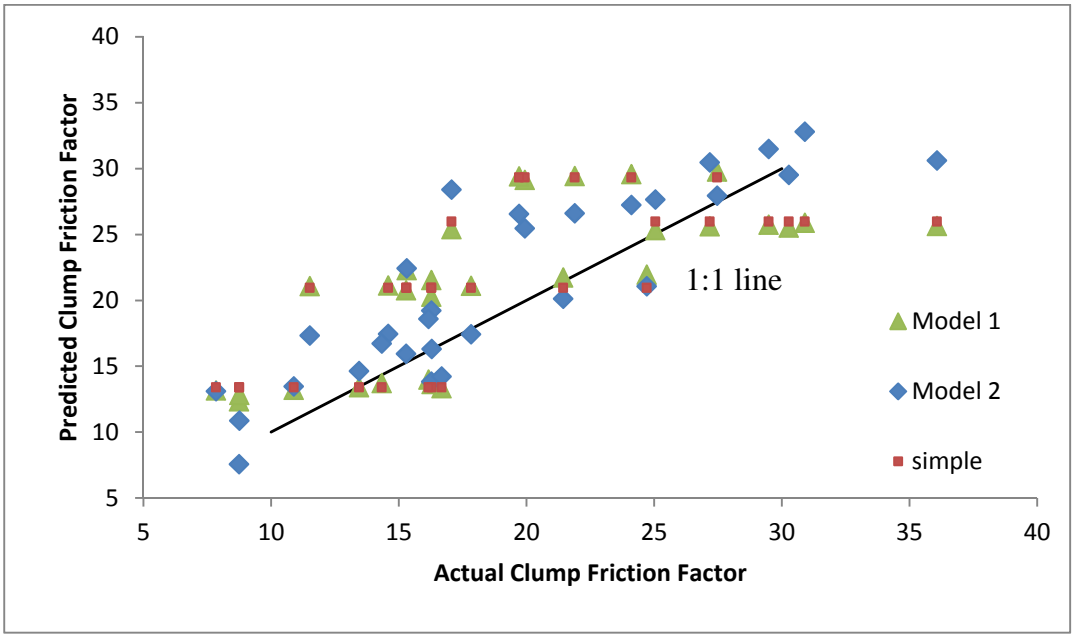

Figure 12. Model 1 - Clump model based on P and the Re_{clump}; Model 2 - Clump model based on P, Re_{rvc}, and the Froude number, Simple Model – Clump model based only on Pclump

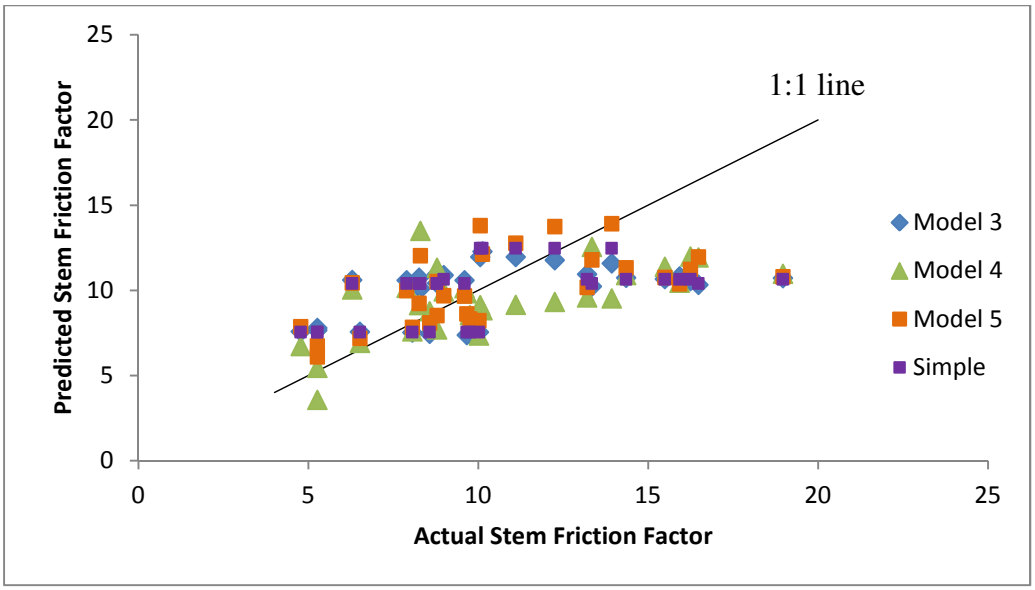

Figure 13. Model 3 - Stem model based on P and Re_{rvs}; Model 4 - Stem model based on P, Re_{rvs}, and Froude number; Model 5 - Stem model based on P, Froude number, and diameter to depth ratio; Simple model – Stem model based only on P_{stem}

The clump regression models had an overall higher R^2 value and matched the 1:1 line better. The regression models using stem data under-predicted friction factor at higher values. The higher friction factors were at the lowest depths where the flow was going around the clumps and not through the stems. The stem models likely do not predict the higher friction factors well because the stems are not influencing those flows. The stem-based models predicted the lower friction factors well where the flow depths were greater and the flow was going both around the clumps and through the stems. The clump-based regression models had good fit throughout the data series, and were overall much better models. A disadvantage to both models is the friction factor becomes negative at high plant densities. Because of this limitation, the highest fraction of vegetated occupied volume suggested for the models is 0.35 and 0.025 for the clump and stem models, respectively.

The R^2 values indicate that even the clump models had only moderately good predictive abilities, likely due to variability in the experimental conditions. Although the study was designed to be fixed bed, small changes in the bed did occur because of the low particle density of the planting medium (discussed in Chapter 3). Other sources of error included plant death and growth throughout the study. The stress of being regularly inundated, a shallow rooting zone, and little to no natural sunlight over the course of the study caused plant stress and death with time. As the plants died, the stems lost some flexibility, which could have affected flow resistance. Due to water surface fluctuations, the water surface elevation was approximated as the average of the low and high surfaces. Also, because of the length of the flume, at low plant densities, the difference in water surface elevation over the length of the flume was close to the measurement error. Additional sources of error include error in measurement of plant frontal area and clump diameter and spacing, due to the natural variability present in studies using real plants.

The clump models are currently specific to the targeted wetlands of the Virginia Piedmont where the growth pattern was observed. For other wetlands types modeling friction factor with stems may be more appropriate. Nepf (1999) saw that wetland vegetation coupled with that flume study grew in a similar formation to that of dowels. While other wetlands besides the Piedmont may have clumping vegetation, the growth pattern of the vegetation of interest should be known before choosing a vegetation resistance model.

Chapter 5. Conclusions

An emergent wetland was recreated in a recirculating flume. Thirty different runs were conducted with four different plant configurations. Flow rate and tailgate height were both changed three times for each plant configuration. Using the measured water surface slope, vegetation friction factors were determined and related to vegetation and flow characteristics. The vegetation characteristic that influenced the friction factor the most was the fraction of plant occupied bed area, P. This value represents the density of the vegetation.

Study results indicated clump density significantly impacts wetland flow, especially at the low depths which are characteristic of emergent wetlands. At low flow depths the water moves around, rather than through, the clumps, due to a dense region of stems at the clump base. At greater depths water flows through the vegetation; however, the occurrence of eddies behind the flow clumps indicates the clumps are a dominant influence on flow resistance. This finding is supported by the formation of sediment deposits behind, rather than within, the clumps.

Over all the models using clump diameter as the representative length scale fit the data better over the full range of the data than models based on stem diameter. Additionally, field measurements of clumps is significantly easier and less time consuming than stem measurements.

The model with the best prediction ability included both vegetation and flow parameters, suggesting flow resistance in wetlands is not exclusively a function of vegetation density. Application of this model will require iteration. If iteration of a

resistance model is not desirable, then a simpler model based only on P could be used, although the model error would be greater.

Future Work

To improve upon the models developed in this study, studies should be conducted with higher plant densities to make the prediction equation more broadly applicable. Creating a model that fits a wide range of P is what is most needed for better model development because it was the most significant parameter throughout the regression analysis. Another consideration to be made would how friction factor might change depending on which calculation form used. Further data analysis using a length scale other than r_v may provide additional insight.

Chapter 6: References

Bedient, P. B., and W. C. Huber. 1992. *Hydrology and floodplain analysis*. 2nd ed. Addison-Wesley, Reading, Mass.

Bennett, S. J., and A. Simon. 2004. *Riparian vegetation and fluvial geomorphology*. American Geophysical Union, Washington, D.C.

Brown, G. O. 2002. The History of the Darcy-Weisbach Equation for Pipe Flow Resistance. R. R. Jerry, and J. F. Augustine, eds: ASCE.

Cheng, N. S., and H. T. Nguyen. 2011. Hydraulic Radius for Evaluating Resistance Induced by Simulated Emergent Vegetation in Open-Channel Flows. *Journal of Hydraulic Engineering-Asce* 137(9):995-1004.

Cole, C. A., and R. P. Brooks. 2000. A comparison of the hydrologic characteristics of natural and created mainstem floodplain wetlands in Pennsylvania. *Ecological Engineering* 14(3):221-231.

Crookshank, S. L., and I. American Petroleum. 1995. *Alternative wetland mitigation programs*. American Petroleum Institute, Washington, D.C.

Cummings, A. R. 1999. An analysis of palustrine mitigation wetlands in the Virginia coastal plain. In *VPI & SU Crop and Soil Environmental Sciences M S 1999*. Blacksburg, Va.: University Libraries, Virginia Polytechnic Institute and State University,.

Dahl, T. E. 1990. *Wetlands losses in the United States, 1780's to 1980's*. U.S. Dept. of the Interior, Fish and Wildlife Service, Washington, D.C.

Dahl, T. E., C. E. Johnson, W. E. Frayer, and U.S. Fish and Wildlife Service. 1991. *Wetlands, status and trends in the conterminous United States, mid-1970's to mid-1980's : first update of the national wetlands status report*. U.S. Dept. of the Interior For sale by the U.S. G.P.O., Supt. of Docs., Washington, D.C.

Donald A, H. 1992. Designing constructed wetlands systems to treat agricultural nonpoint source pollution. *Ecological Engineering* 1(1–2):49-82.

Dugan, P., Mitchell Beazley Ltd., and International Union for Conservation of Nature and Natural Resources. 1993. Wetlands in danger : a world conservation atlas. New York: Oxford University Press,.

Garbisch, E. W. 2002. *The do's and don'ts of wetland construction : creation, restoration, and enhancement*. Environmental Concern, St. Michael's, MD.

Jarvela, J. 2002. Flow resistance of flexible and stiff vegetation: a flume study with natural plants. *Journal of Hydrology* 269(1-2):44-54.

Järvelä, J. 2004. Determination of flow resistance caused by nonsubmerged woody vegetation. *International Journal of River Basin Management* 2(1):61-70.

Jiang, M., X. G. Lu, L. S. Xu, L. J. Chu, and S. Z. Tong. 2007. Flood mitigation benefit of wetland soil - A case study in momoge national nature reserve in China. *Ecological Economics* 61(2-3):217-223.

Kadlec, R. H. 1990. Overland-Flow in Wetlands - Vegetation Resistance. *Journal of Hydraulic Engineering-Asce* 116(5):691-706.

Liu, D., P. Diplas, J. D. Fairbanks, and C. C. Hodges. 2008. An experimental study of flow through rigid vegetation. *Journal of Geophysical Research-Earth Surface* 113(F4).

Maltby, E., T. Barker, and Wiley online library. 2009. The wetlands handbook. In *Replumbing Wetlands - Managing water for the restoration of bogs and fens*. Chichester, UK ; Hoboken, NJ: Wiley-Blackwell.

Mitsch, W. J., and J. G. Gosselink. 2000. *Wetlands*. 3rd ed. John Wiley, New York.

National Research Council . Committee on Mitigating Wetland, L. 2001. *Compensating for wetland losses under the Clean Water Act*. National Academy Press, Washington, D.C.

Nepf, H. M. 1999. Drag, turbulence, and diffusion in flow through emergent vegetation. *Water Resources Research* 35(2):479-489.

Piercy, C. D. 2010. Hydraulic resistance due to emergent wetland vegetation. Blacksburg, Va.: University Libraries, Virginia Polytechnic Institute and State University,.

Roig, L. C. 1994. Hydrodynamic modeling of flows in tidal wetlands. University of California, Davis, Civil and Environmental Engineering

Rolf H. Sabersky, A. J. A., Edward G. Hauptmann, E. M. Gates. 1999. *Fluid Flow: A First Course in Fluid Mechanics*. 4 ed. Prentice Hall Inc.

Sand-Jensen, K. 2003. Drag and reconfiguration of freshwater macrophytes. *Freshwater Biology* 48(2):271-283.

Strand, M. N., L. Rothschild, and Environmental Law Institute. 2009. *Wetlands deskbook*. 3rd ed. ELI Press, Environmental Law Institute, Washington, D.C.

Strausbaugh, P. D., and E. L. Core. 1978. *Flora of West Virginia*. 2d ed. Seneca Books, Grantsville, W. Va.

Appendix A. K_s Determination

Table 8 A1. Cross section data used to determine ks

Cross Section 1			Cross Section 2			Cross Section 3		
x (cm)	y (mm)	Heights (mm)	x (cm)	y (mm)	Heights (mm)	x (cm)	y (mm)	Heights (mm)
100	63.97	16.4	100	63.24	14.07	100	66.81	17.19
95	64.3	16.73	95	60.15	10.98	95	65.78	16.16
90	65.02	17.45	93	58.68	9.51	90	62.58	12.96
85	60.26	12.69	90	53.02	3.85	85	60	10.38
80	56.77	9.2	85	53.58	4.41	80	57.59	7.97
75	57.22	9.65	80	51.84	2.67	75	53.05	3.43
70	57.14	9.57	75	55.89	6.72	70	56.24	6.62
67	62.06	14.49	70	58.71	9.54	65	59.06	9.44
65	57.88	10.31	65	56.08	6.91	63	57.34	7.72
60	47.57	0	60	49.17	0	60	53.33	3.71
55	52.07	4.5	55	50.7	1.53	55	49.62	0
50	59.15	11.58	50	57.07	7.9	52	57.16	7.54
45	62.82	15.25	45	56.56	7.39	50	56.25	6.63
40	58.14	10.57	40	59.33	10.16	45	54.73	5.11
35	60.34	12.77	35	61.13	11.96	40	58.71	9.09
30	58.83	11.26	30	53.14	3.97	35	56.67	7.05
25	58.58	11.01	25	53.21	4.04	30	55.51	5.89
20	61.26	13.69	20	63.53	14.36	25	56.48	6.86
						20	58.61	8.99

Table 9 A2. Frequency distribution used to find ks

Bin	*Frequency*	*Cumulative %*
1	3	5.45%
2	1	7.27%
3	1	9.09%
4	4	16.36%
5	3	21.82%
6	2	25.45%
7	5	34.55%
8	6	45.45%
9	1	47.27%
10	7	60.00%
11	5	69.09%
12	4	76.36%
13	3	81.82%
14	1	83.64%
15	3	89.09%
16	1	90.91%
17	3	96.36%
18	2	100.00%

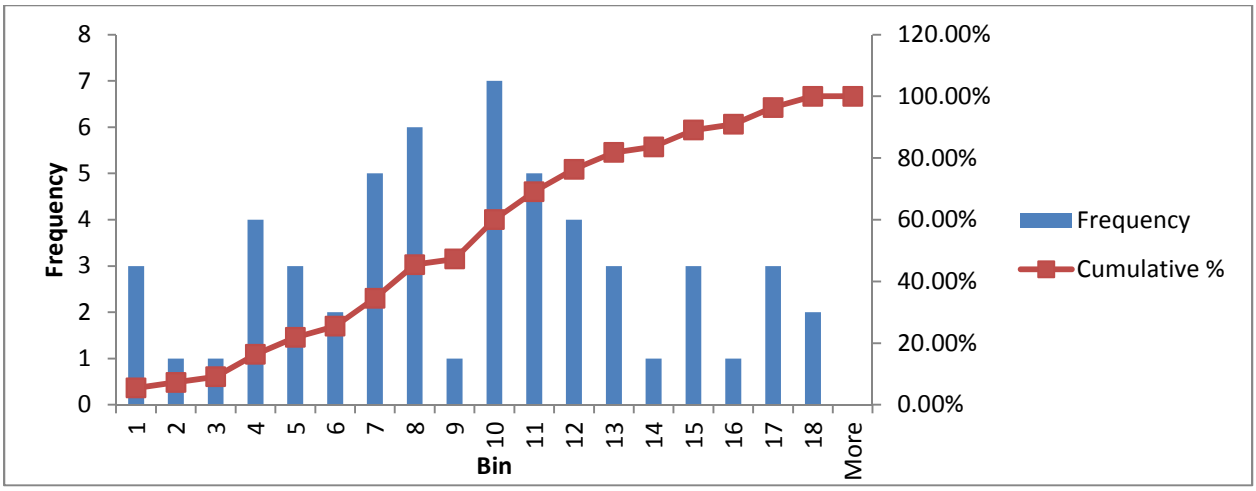

Figure A1. Histogram and frequency plot used to determine k_s

Appendix B: Corrections

Table 10 B1. Clump based friction factor corrections

Flow Rate (L/s)	Spacing (cm)	Diameter (cm)	Tailgate Height (cm)	r_v (m)	Re	f	f_s	f_{rw}	α_w	f_w	f_{rb}	α_b	f_b	r_{vm}	f_{vm}
3	25	12	2.5	0.46	13363	2.07	0.08	0.01	7.71	0.08	0.34	2.46	0.34	0.39	21.43
4	25	12	2.5	0.46	17487	2.82	0.08	0.01	7.63	0.08	0.36	2.44	0.37	0.41	24.71
5	25	12	2.5	0.46	21568	1.99	0.07	0.01	8.00	0.07	0.27	2.56	0.28	0.40	15.30
3	25	12	7.5	0.46	12605	2.51	0.09	0.01	7.97	0.09	0.28	2.55	0.29	0.41	16.27
4	25	12	7.5	0.46	16698	2.46	0.08	0.01	8.03	0.08	0.27	2.57	0.27	0.41	15.29
5	25	12	7.5	0.46	20631	3.04	0.08	0.01	7.92	0.08	0.29	2.53	0.30	0.42	17.83
3	25	12	5	0.46	13122	1.38	0.07	0.01	8.20	0.07	0.24	2.62	0.24	0.38	11.51
4	25	12	5	0.46	16996	2.11	0.08	0.01	8.05	0.08	0.27	2.57	0.27	0.41	14.58
5	25	12	5	0.46	21040	2.49	0.08	0.01	7.97	0.08	0.28	2.55	0.28	0.41	16.27
3	20	12	7.5	0.28	13942	2.36	0.08	0.01	8.06	0.08	0.26	2.58	0.27	0.25	8.74
4	20	12	7.5	0.28	18439	2.47	0.08	0.01	8.07	0.08	0.26	2.58	0.27	0.25	8.75
5	20	12	7.5	0.28	22799	3.22	0.08	0.01	7.90	0.08	0.29	2.53	0.30	0.25	10.88
3	20	12	5	0.28	14526	1.63	0.07	0.01	8.11	0.07	0.26	2.59	0.26	0.23	7.84
4	20	12	5	0.28	18940	3.17	0.08	0.01	7.73	0.08	0.34	2.47	0.34	0.25	13.43
5	20	12	5	0.28	23315	3.71	0.08	0.01	7.69	0.08	0.35	2.46	0.35	0.25	14.33
3	20	12	2.5	0.28	14607	3.16	0.09	0.01	7.55	0.09	0.39	2.41	0.39	0.24	16.67
4	20	12	2.5	0.28	19115	3.57	0.09	0.01	7.58	0.09	0.38	2.42	0.38	0.25	16.28
5	20	12	2.5	0.28	23556	3.91	0.08	0.01	7.59	0.08	0.37	2.43	0.38	0.25	16.16
3	20	8	2.5	0.49	12396	2.66	0.09	0.01	7.60	0.09	0.37	2.43	0.38	0.43	27.18
4	20	8	2.5	0.49	16094	4.35	0.10	0.01	7.42	0.10	0.43	2.37	0.44	0.45	36.08

Table B1, cont. Clump based friction factor corrections

Flow Rate (L/s)	Spacing (cm)	Diameter (cm)	Tailgate Height (cm)	r_v (m)	Re	f	f_s	f_{rw}	α_w	f_w	f_{rb}	α_b	f_b	r_{vm}	f_{vm}
5	20	8	2.5	0.49	19884	4.07	0.09	0.01	7.54	0.09	0.39	2.41	0.40	0.45	30.89
3	20	8	5	0.49	12194	2.84	0.09	0.01	7.68	0.09	0.35	2.45	0.35	0.44	25.04
4	20	8	5	0.49	15976	3.87	0.09	0.01	7.55	0.09	0.39	2.41	0.39	0.45	30.28
5	20	8	5	0.49	19717	4.10	0.09	0.01	7.58	0.09	0.38	2.42	0.38	0.45	29.48
5	20	8	7.5	0.49	19219	2.81	0.08	0.01	8.00	0.08	0.27	2.56	0.28	0.45	17.06
4	25	8	5	0.77	15424	1.63	0.07	0.01	8.19	0.07	0.24	2.62	0.25	0.66	19.94
5	25	8	5	0.77	19127	1.88	0.07	0.01	8.13	0.07	0.25	2.60	0.26	0.67	21.89
3	25	8	2.5	0.77	12029	1.18	0.07	0.01	8.14	0.07	0.25	2.60	0.25	0.61	19.70
4	25	8	2.5	0.77	15774	1.64	0.07	0.01	8.02	0.07	0.27	2.56	0.27	0.65	24.10
5	25	8	2.5	0.77	19447	2.07	0.07	0.01	7.94	0.07	0.29	2.54	0.29	0.67	27.46

Table 11B2. Stem based friction factor corrections

Flow Rate (L/s)	Spacing (cm)	Diameter (cm)	Tailgate Height (cm)	rv (m)	Re	f	f_s	f_{rw}	α_w	f_w	f_{rb}	α_b	f_b	r_{vm}	f_{vm}
3	25	12	2.5	0.25	11236	2.93	0.10	0.01	7.45	0.10	0.42	2.38	0.43	0.21	16.49
4	25	12	2.5	0.25	14703	3.98	0.10	0.01	7.37	0.10	0.45	2.36	0.46	0.22	13.35
5	25	12	2.5	0.25	18135	2.82	0.08	0.01	7.73	0.08	0.34	2.47	0.34	0.22	8.31
3	25	12	7.5	0.25	10598	3.56	0.10	0.01	7.70	0.10	0.34	2.46	0.35	0.22	8.79
4	25	12	7.5	0.25	14040	3.48	0.09	0.01	7.75	0.09	0.33	2.48	0.34	0.22	8.26
5	25	12	7.5	0.25	17346	4.30	0.09	0.01	7.65	0.09	0.36	2.44	0.36	0.23	9.61
3	25	12	5	0.25	11033	1.95	0.08	0.01	7.92	0.08	0.29	2.53	0.30	0.21	6.30
4	25	12	5	0.25	14291	2.99	0.09	0.01	7.78	0.09	0.32	2.49	0.33	0.22	7.90

Table B2, cont. Stem based friction factor corrections

Flow Rate (L/s)	Spacing (cm)	Diameter (cm)	Tailgate Height (cm)	rv (m)	Re	f	f_s	f_{rw}	α_w	f_w	f_{rb}	α_b	f_b	r_{vm}	f_{vm}
5	25	12	5	0.25	17690	3.52	0.09	0.01	7.70	0.09	0.34	2.46	0.35	0.22	8.79
3	20	12	7.5	0.16	10592	4.09	0.11	0.01	7.63	0.11	0.36	2.44	0.37	0.15	5.27
4	20	12	7.5	0.16	14008	4.29	0.10	0.01	7.63	0.10	0.36	2.44	0.37	0.15	5.27
5	20	12	7.5	0.16	17320	5.59	0.10	0.01	7.48	0.10	0.41	2.39	0.42	0.15	6.52
3	20	12	5	0.16	11035	2.82	0.09	0.01	7.67	0.09	0.35	2.45	0.36	0.14	4.79
4	20	12	5	0.16	14389	5.49	0.11	0.01	7.31	0.11	0.48	2.34	0.49	0.15	8.07
5	20	12	5	0.16	17712	6.43	0.11	0.01	7.28	0.11	0.50	2.33	0.50	0.15	8.58
3	20	12	2.5	0.16	11097	5.47	0.12	0.01	7.14	0.12	0.57	2.28	0.58	0.15	10.02
4	20	12	2.5	0.16	14522	6.19	0.11	0.01	7.17	0.11	0.55	2.29	0.56	0.15	9.76
5	20	12	2.5	0.16	17896	6.77	0.11	0.01	7.19	0.11	0.54	2.30	0.55	0.15	9.67
3	20	8	2.5	0.26	11126	3.31	0.10	0.01	7.44	0.10	0.43	2.38	0.43	0.23	14.35
4	20	8	2.5	0.26	14445	5.40	0.11	0.01	7.26	0.11	0.50	2.32	0.51	0.24	18.97
5	20	8	2.5	0.26	17846	5.05	0.10	0.01	7.38	0.10	0.45	2.36	0.46	0.24	16.24
3	20	8	5	0.26	10944	3.52	0.10	0.01	7.51	0.10	0.40	2.40	0.41	0.23	13.21
4	20	8	5	0.26	14339	4.81	0.10	0.01	7.39	0.10	0.45	2.36	0.45	0.24	15.93
5	20	8	5	0.26	17696	5.09	0.10	0.01	7.42	0.10	0.44	2.37	0.44	0.24	15.50
5	20	8	7.5	0.26	17249	3.49	0.09	0.01	7.83	0.09	0.31	2.50	0.32	0.24	8.99
4	25	8	5	0.39	14375	1.88	0.08	0.01	8.08	0.08	0.26	2.58	0.26	0.34	10.13
5	25	8	5	0.39	17825	2.16	0.08	0.01	8.02	0.08	0.27	2.56	0.28	0.34	11.11
3	25	8	2.5	0.39	11211	1.35	0.08	0.01	8.02	0.08	0.27	2.56	0.27	0.31	10.07
4	25	8	2.5	0.39	14700	1.89	0.08	0.01	7.91	0.08	0.29	2.53	0.30	0.33	12.26
5	25	8	2.5	0.39	18123	2.38	0.08	0.01	7.83	0.08	0.31	2.50	0.31	0.34	13.93

Appendix C: Minitab Outputs

Clump Regression:

Initial run including all the parameters:

```
* MAA*D is highly correlated with other X variables
* MAA*D has been removed from the equation.


The regression equation is
FF_Cl = 25.6 - 133 Cl_Porosity - 0.000504 Ch_Re_Cl + 2.79 D/H + 1396 Fr
        - 0.000409 Buck_Re_Cl


Predictor          Coef    SE Coef      T      P    VIF
Constant         25.595      7.304   3.50  0.002
Cl_P           -133.34      32.09  -4.15  0.000  9.448
Ch_Re_Cl     -0.0005041  0.0001281  -3.94  0.001  7.980
D/H               2.786      2.118   1.32  0.201  1.834
Fr               1395.7      279.5   4.99  0.000  3.514
Buck_Re_Cl   -0.0004091  0.0007324  -0.56  0.582  4.885
```

MAA*D was highly correlated with Cl_P. Another run was done removing P to compare outputs.

```
The regression equation is
FF_Cl = 25.6 - 0.000504 Ch_Re_Cl + 2.79 D/H - 105 MAA*D + 1396 Fr
        - 0.000409 Buck_Re_Cl


Predictor          Coef    SE Coef      T      P    VIF
Constant         25.595      7.304   3.50  0.002
Ch_Re_Cl    -0.0005041  0.0001281  -3.94  0.001  7.980
D/H               2.786      2.118   1.32  0.201  1.834
MAA*D          -104.67      25.19  -4.15  0.000  9.448
Fr               1395.7      279.5   4.99  0.000  3.514
Buck_Re_Cl  -0.0004091  0.0007324  -0.56  0.582  4.885


S = 3.78002   R-Sq = 80.8%   R-Sq(adj) = 76.8%

PRESS = 542.493   R-Sq(pred) = 69.66%
```

The results were identical in terms of model performance.

Determining best models

Vars	R-Sq	R-Sq(adj)	Mallows Cp	S	Cl_Porosity	Ch_Res_Cl	D/H	Fr	Buck_Res_Cl
1	58.0	56.5	26.6	5.1810	X				
1	38.0	35.8	51.5	6.2902				X	
1	34.2	31.9	56.3	6.4818		X			
1	16.6	13.6	78.3	7.2970					X
1	6.6	3.2	90.9	7.7250			X		
2	65.5	62.9	19.2	4.7826	X			X	
2	64.6	61.9	20.4	4.8450				X	X
2	58.4	55.3	28.0	5.2478	X				X
2	58.3	55.2	28.2	5.2543	X	X			
2	58.0	54.9	28.6	5.2752	X		X		
3	79.4	77.1	3.7	3.7615	X	X		X	
3	68.0	64.3	18.1	4.6928	X			X	X
3	65.9	61.9	20.7	4.8449			X	X	X
3	65.6	61.6	21.0	4.8637	X		X	X	
3	65.0	61.0	21.7	4.9032		X		X	X
4	80.6	77.5	4.3	3.7276	X	X	X	X	
4	79.4	76.2	5.7	3.8348	X	X		X	X
4	68.4	63.4	19.5	4.7506	X		X	X	X
4	67.0	61.8	21.3	4.8563		X	X	X	X
4	60.9	54.6	28.9	5.2890	X	X	X		X
5	80.8	76.8	6.0	3.7800	X	X	X	X	X

Analysis of best models

Model 1:

```
The regression equation is
FF_Cl = 34.5 - 94.9 Cl_Porosity + 0.000312 Buck_Re_Cl


Predictor          Coef    SE Coef      T      P    VIF
Constant         34.489      3.841   8.98  0.000
Cl_Porosity     -94.89      18.22  -5.21  0.000  1.579
Buck_Re_Cl   0.0003120  0.0005781   0.54  0.594  1.579


S = 5.24782   R-Sq = 58.4%   R-Sq(adj) = 55.3%

PRESS = 898.848   R-Sq(pred) = 49.74%
```

Model 2:

```
The regression equation is
FF_Cl = 28.5 - 133 Cl_Porosity - 0.000473 Ch_Re_Cl + 1284 Fr


Predictor          Coef    SE Coef      T      P    VIF
Constant         28.542      5.941   4.80  0.000
Cl_Porosity     -132.71      19.04  -6.97  0.000  3.359
Ch_Re_Cl     -0.0004730  0.0001126  -4.20  0.000  6.227
Fr               1283.5      248.5   5.17  0.000  2.805


S = 3.76152   R-Sq = 79.4%   R-Sq(adj) = 77.1%

PRESS = 489.470   R-Sq(pred) = 72.63%
```

Stem Regression

Initial run including all the parameters:

```
* Buck_Re_St is highly correlated with other X variables
* Buck_Re_St has been removed from the equation.


* St_Porosity is highly correlated with other X variables
* St_Porosity has been removed from the equation.


The regression equation is
FF_St = 13.2 + 42.1 D/H - 785 MAA*D - 0.000715 Ch_Re_St + 175 Fr


Predictor        Coef    SE Coef      T      P    VIF
Constant       13.206      3.857   3.42  0.002
D/H             42.05      34.73   1.21  0.237  1.302
MAA*D          -785.4      148.5  -5.29  0.000  4.462
Ch_Re_St   -0.0007146  0.0001778  -4.02  0.000  9.080
Fr             174.67      42.41   4.12  0.000  3.634


S = 2.34438   R-Sq = 65.5%   R-Sq(adj) = 60.0%

PRESS = 205.126   R-Sq(pred) = 48.48%
```

MAA*D was highly correlated with Cl_P. Buck_Re_St was highly correlated with Fr, so another run was done without Fr.

```
The regression equation is
FF_St = 13.2 - 1001 St_Porosity - 0.000715 Ch_Re_St + 42.1 D/H
        + 0.0731 Buck_Re_St


Predictor          Coef    SE Coef      T      P    VIF
Constant         13.206      3.857   3.42  0.002
St_Porosity     -1000.5      189.2  -5.29  0.000  4.462
Ch_Re_St     -0.0007146  0.0001778  -4.02  0.000  9.080
D/H              42.05      34.73   1.21  0.237  1.302
Buck_Re_St      0.07310    0.01775   4.12  0.000  3.634
```

```
S = 2.34438   R-Sq = 65.5%   R-Sq(adj) = 60.0%

PRESS = 205.126   R-Sq(pred) = 48.48%
```

Determining best models:

Vars	R-Sq	R-Sq(adj)	Mallows Cp	S	Fr	D/H	Ch_Re_St	St_Porosity
1	36.8	34.6	19.8	2.9971				X
1	23.6	20.8	29.4	3.2964	X			
1	20.7	17.9	31.4	3.3579			X	
1	12.8	9.7	37.2	3.5212		X		
2	42.4	38.1	17.8	2.9154	X			X
2	39.7	35.2	19.7	2.9818		X		X
2	37.5	32.9	21.2	3.0348			X	X
2	26.0	20.5	29.6	3.3038	X	X		
2	25.1	19.5	30.3	3.3237	X		X	
3	63.5	59.2	4.5	2.3653	X		X	X
3	43.2	36.6	19.2	2.9497	X	X		X
3	42.1	35.4	20.0	2.9784		X	X	X
3	26.9	18.5	31.0	3.3458	X	X	X	
4	65.5	60.0	5.0	2.3444	X	X	X	X

Analysis of best models:

Model 3:

```
The regression equation is
FF_St = 18.6 - 558 St_Porosity - 0.000076 Ch_Re_St


Predictor          Coef    SE Coef      T      P    VIF
Constant         18.556      4.593   4.04  0.000
St_Porosity      -557.6      206.7  -2.70  0.012  3.176
Ch_Re_St     -0.0000755  0.0001361  -0.55  0.584  3.176


S = 3.03483   R-Sq = 37.5%   R-Sq(adj) = 32.9%

PRESS = 296.863   R-Sq(pred) = 25.43%
```

Model 4:

```
The regression equation is
FF_St = 14.7 - 998 St_Porosity - 0.000691 Ch_Re_St + 182 Fr


Predictor          Coef    SE Coef      T      P    VIF
Constant         14.681      3.692   3.98  0.000
St_Porosity      -997.7      190.9  -5.23  0.000  4.461
Ch_Re_St     -0.0006909  0.0001783  -3.88  0.001  8.970
Fr               181.93      42.36   4.30  0.000  3.562


S = 2.36529   R-Sq = 63.5%   R-Sq(adj) = 59.2%

PRESS = 192.856   R-Sq(pred) = 51.56%
```

Model 5:

```
The regression equation is
FF_St = 8.65 - 359 St_Porosity + 42.5 Fr + 26.7 D/H


Predictor      Coef  SE Coef      T      P    VIF
Constant      8.649    4.638   1.86  0.074
St_Porosity  -359.2    128.0  -2.81  0.009  1.290
Fr            42.52    33.71   1.26  0.218  1.450
D/H           26.66    43.44   0.61  0.545  1.286


S = 2.94969   R-Sq = 43.2%   R-Sq(adj) = 36.6%

PRESS = 302.324   R-Sq(pred) = 24.06%
```

Appendix D: Prediction equation results for friction factors that incorporate bed and vegetation effects

The prediction equations found for the clump and stem models had the same parameters as the models that incorporated both vegetation and bed effects. Model coefficients were different. Prediction equations that were found by Minitab are reported below along with the PRESS Statistic and R^2 values for each model.

Clump Models

Table 12D1. Clump friction factor prediction equations with incorporated bed roughness

Model Number	Equation	R^2	Press
Simple	$f = 36.8 - (91 \times P)$	56.9	930
1	$f = 35.2 - (97.2 \times P) + (0.000327 \times Re_{clump})$	57.4	981
2	$f = 29.1 - (137 \times P) - (0.000495 \times Re_{rv}) + (1339 \times Fr)$	78.9	534

* P is plant occupied bed area, Fr if Froude number, Re_{rv} is the Reynolds number where the length scale is r_{vc}, and Re_{clump} is the Reynolds number found from the Buckingham Pi analysis (length scale is clump diameter)

Stem Models

Table 13D2. Stem friction factor prediction equations with incorporated bed roughness

Model Number	Equation	R^2	Press
Simple	$f = 19.3 - (282 \times P)$	10.8	517
3	$f = 14.7 - (958 \times P) - (0.000903 \times Re_{Rv}) + (251 \times Fr)$	49.7	339
4	$f = 8.12 - (127 \times P) + (70.5 \times Fr) + (27.3 \times {}^{D}/_{H})$	22.1	512

* P is plant occupied bed area, Fr if Froude number, Re_{rv} is the Reynolds number where the length scale is r_{vs}, and D/H is the diameter to water depth ratio